ISSN 0280-5316
ISRN LUTFD2/TFRT--5703--SE

Diabetes Mellitus Modelling Based on Blood Glucose Measurements

Fredrik Ståhl

Department of Automatic Control
Lund Institute of Technology
April 2003

Department of Automatic Control
Lund Institute of Technology
Box 118
SE-221 00 Lund Sweden

Document name
MASTER THESIS

Date of issue
April 2003

Document Number
ISRN LUTFD2/TFRT--5703--SE

Author(s)
Fredrik Ståhl

Supervisor
Rolf Johansson, LTH
Christian Liisberg at Nova Nordisk AS, Denmark
Mona Landin-Olsson, Med.Klinic at Lund University Hospital.

Sponsoring organization

Title and subtitle
Diabetes Mellitus Modelling Based on Blood Glucose Measurements. (Diabetes Mellitus-modellering baserad på blodglukosdata).

Abstract
Insulin Dependant Diabetes Mellitus(IDDM) is a chronic disease characterized by the inability of the pancreas to produce sufficient amounts of insulin. To cover the deficiency 4-6 insulin injections have to be taken daily. The aim of this insulin therapy is to maintain normoglycemia, blood glucose level between 4-7 mmol/L. To determine the amount and timing of these injections different approaches are used. Mostly qualitative and semiquantitative models and reasoning are used to design such a therapy. In this Master Thesis an attempt is made to show how system identification and automatic control perspectives may be used to estimate quantitative models. Such models can then be used to design optimal insulin regimens. The system was divided into three subsystems, the insulin subsystem, the glucose subsystem and the insulin/glucose interaction. The insulin subsystem aims to describe the absorption of injected insulin from the subcutaneous depots and the glucose subsystem the absorption of glucose from the gut following a meal. These subsystems were modelled using compartment models and proposed models found in the literature. Several black box models and grey-box models describing the insulin/glucose interaction have been developed and analysed. These models have been fitted to real data monitored by a IDDM patient. Many difficulties were encountered, typical of biomedical systems. Non-uniform and scarce sampling, time-varying dynamics and severe non-linearities were some of the difficulties encountered during the modelling. None of the proposed models were able to describe the system accurately. However, all the linear models shared some dynamics, and there is ground to suspect that these dynamics are essential parts of the true system. More research has to be undertaken, primarily to investigate the non-linear nature of the system and to see whether other variables than glucose flux and insulin absorption are important for the dynamics of the system.

Keywords
Keywords: diabetes, mathematical model, identification, glucose dynamics, insulin dynamics.

Classification system and/or index terms (if any)

Supplementary bibliographical information

ISSN and key title
0280-5316

ISBN

Language
English

Number of pages
91

Recipient's notes

Security classification

Diabetes Mellitus Modelling Based On Blood Glucose Measurements

F. Ståhl

April 17, 2003

Abstract

Insulin Dependant Diabetes Mellitus(IDDM) is a chronic disease characterized by the inability of the pancreas to produce sufficient amounts of insulin. To cover the deficiency 4-6 insulin injections have to be taken daily. The aim of this insulin therapy is to maintain normoglycemia, blood glucose level between 4-7 mmol/L. To determine the amount and timing of these injections different approaches are used. Mostly qualitative and semi-quantitative models and reasoning are used to design such a therapy. In this Master Thesis an attempt is made to show how system identification and automatic control perspectives may be used to estimate quantitative models. Such models can then be used to design optimal insulin regimens.

The system was divided into three subsystems, the insulin subsystem, the glucose subsystem and the insulin/glucose interaction. The insulin subsystem aims to describe the absorbtion of injected insulin from the subcutaneous depots and the glucose subsystem the absorbtion of glucose from the gut following a meal. These subsystems were modelled using compartment models and proposed models found in the literature. Several black box models and grey-box models describing the insulin/glucose interaction have been developed and analysed. These models have been fitted to real data monitored by a IDDM patient. Many difficulties were encountered, typical of biomedical systems. Non-uniform and scarce sampling, time-varying dynamics and severe non-linearities were some of the difficulties encountered during the modelling. None of the proposed models were able to describe the system accurately. However, all the linear models shared some dynamics, and there is ground to suspect that these dynamics are essential parts of the true system. More research has to be undertaken, primarily to investigate the non-linear nature of the system and to see whether other variables than glucose flux and insulin absorbtion are important for the dynamics of the system.

Keywords: diabetes, mathematical model, identification, glucose dynamics, insulin dynamics.

Sammanfattning

Diabetes Mellitus typ 1(IDDM) är en kronisk sjukdom karaktäriserad av oförmågan att producera eget insulin i tillräcklig utsträckning. För att täcka denna förlust måste 4-6 insulin injektioner tas varje dag. Syftet med en sådan terapi är att bibehålla normala blodglukosvärden, som ligger mellan 4-7mmol/l. Olika ansatser används för att bestämma storleken och tidpunkten för insulindoserna. Huvudsakligen beaktas semi-kvantitativa modeller och resonemang för att fastställa en sådan insulinregim. Syftet med det här examensarbetet är att utveckla kvantitativa modeller, som ska kunna användas i utvecklingen av optimala regleringsprinciper för insulin-injektionerna.

Systemet delas upp i tre delsystem, insulinsubsystemet, glukossubsystemet och glukos/insulin-interaktionssystemet(GIIM). Insulinsubsystemet beskriver hur insulinet absorberas från de subkutana vävnaderna efter en insulin-injektion. Glukossubsystemet syftar till att beskriva glukosflödet från matsmältningsapparaten efter en måltid. Dessa subsystem har modellerats med compartmentmodeller, samt modeller funna i litteraturen. GIIM har modellerats huvudsakligen med black-box-modeller, som skattats på verkligt uppmätt data från en IDDM-patient. Många svårigheter, typiska för biologiska system, döck upp. Icke-ekvidistant och lågfrekvent sampling, tids-varierande dynamik och svåra olinjäriteter är några av de problem som påträffades. Ingen av de föreslagna modellerna kunde beskriva systemet särskilt väl, men samtliga linjära modeller hade vissa gemensamma drag. Det finns därför viss grund att tro att dessa drag är essentiella för det verkliga systemet. Mer forskning krävs, främst för att analysera systemets olinjära natur, men även för att utröna om och hur andra variabler än glukos och insulinintag påverkar systemet.

Nyckelord: diabetes, matematisk modell, identifiering, glukos dynamik, insulin dynamik.

Acknowledgements

First I would like to express my gratitude towards my three supervisors; Rolf Johansson, Christian Liisberg and Mona Landin-Olsson for their guidance and many helpful discussions. I would also like to thank Per Hagander at the department of Automatic Control, LTH for his interest and help in providing contacts and Jette Randløv and Jon Hansen at Novo Nordisk for literature suggestions and valuable comments on the preliminary manuscript. My warmest thanks goes to my friends and family for their love and support during these months, especially my girlfriend Åsa Bergman and my close friend Fredrik Ehrnford. I am also grateful to Novo Nordisk for providing the MiniMod data and for the financial support.

Preface

In January 2002 I was diagnosed Diabetes Type 1. I soon realized the difficulty of maintaining normoglycemia. This spurred me to investigate whether control theory could be applied to the problem. To analyze the system using the tools of automatic control, a model of the system is however essential. This thesis is an attempt to estimate such a model based on home monitored data, typically found in a diabetes diary. The models used were primarily linear and were found to be insufficient to describe the system. Future research, especially the physiological models may hopefully better describe the system. Such models together with some robust control algorithm may constitute a helpful decision support tool, making life easier for millions of people.

Fredrik Ståhl
Lund
April 17, 2003

List of Symbols and Abbreviations

List of Symbols

Greek Letters		
Symbol	**Description**	**Units**
η	Absorbtion efficiency	[-]
Γ_{fast}	Γ-matrix of the disc. fast carb comp. model	[-]
Γ_{Hum}	Γ-matrix of the disc. Humalog comp. model	[-]
Γ_{slow}	Γ-matrix of the disc. slow carb comp. model	[-]
Φ_{fast}	Φ-matrix of the disc. fast carb comp. model	[-]
Φ_{Hum}	Φ-matrix of the disc. Humalog comp. model	[-]
Φ_{slow}	Φ-matrix of the disc. slow carb comp. model	[-]
Roman Letters		
Symbol	**Description**	**Units**
a	Constant in Ackerman's model	$[min^{-1}]$
a_{50}	Constant in Berger's model	[min/U]
A	A-matrix of the extended Ack. model	[-]
$A(z^{-1})$	Output Polynomial in ARMAX etc.	[-]
$A_{fast}(z^{-1}$	Denominator of the fast carb. comp. model's tf	[-]
$A_{Hum}(z^{-1}$	Denominator of the Humalog comp. model's tf	[-]
$A_{slow}(z^{-1}$	Denominator of the slow carb. comp. model's tf	[-]
$A(t)$	Amount(%) insulin remaining in depot at time t	[-]
A_{fast}	A-matrix of the fast carb. comp. model	[-]
A_{Hum}	A-matrix of the Humalog comp. model	[-]
A_{slow}	A-matrix of the slow carb. comp. model	[-]
b	Constant in Ackerman's model	$[mmol \cdot U^{-1} \cdot min^{-1}]$
b_{50}	Constant in Berger's model	[min/U]
B	B-matrix of the extended Ack. model	[-]
$B(z^{-1})$	Input i:s Polynomial in ARMAX etc.	[-]
$B_{fast}(z^{-1}$	Numerator of the fast carb. comp. model's tf	[-]
$B_{Hum}(z^{-1}$	Numerator of the Humalog comp. model's tf	[-]
$B_{slow}(z^{-1}$	Numerator of the slow carb. comp. model's tf	[-]
B_{fast}	B-matrix in the fast carb. comp. model	[-]
B_{Hum}	B-matrix in the Humalog comp. model	[-]
B_{slow}	B-matrix in the slow carb. comp. model	[-]

List of Symbols(continued)

Symbol	Description	Units
c	Constant in Ackerman's model	$[mmol^{-1} \cdot U \cdot min^{-1}]$
c_0	Artificial Rate coeff. in comp. model	[-]
c_i	Rate coeff. in comp. model, out from comp. i	[-]
c_{ij}	Rate coeff. in comp. model, from comp. i to j	[-]
C	C-matrix of the extended Ack. model	[-]
$C(z^{-1})$	Noise Polynomial in ARMAX etc.	[-]
C_{fast}	C-matrix of the fast carb. comp. model	[-]
C_{Hum}	C-matrix of the Humalog comp. model	[-]
C_{slow}	C-matrix of the slow carb. comp. model	[-]
d	Constant in Ackerman's model	$[min^{-1}]$
d_{ij}	Rate coeff. in discrete comp. model, from comp. i to j	[-]
D	D-matrix of the extended Ack. model	[-]
$D(z^{-1})$	Noise Polynomial in GTFM	[-]
$e(k)$	White noise	[mmol/l]
f_{max}	Maximum frequency of interest	[Hz]
f_s	Sampling frequency	[Hz]
$F(z^{-1})$	Input i:s polynomial in GTFM	[-]
$C_{fast,k}$	Amount of Ingested Fast Carbohydrates at t_k	[g]
$C_{slow,k}$	Amount of Ingested Slow Carbohydrates at t_k	[g]
$D_{Hum,k}$	Amount of Injected Humalog at t_k	[U]
$D_{IT,k}$	Amount of Injected Humalog at t_k	[U]
$f_{sub_{IT}}(t)$	Berger function of insulin abs.	$[l^{-1}]$
$G_{in}(t)$	Total Glucose flux	[mmol/l]
$G_{in_{fast}}(t)$	Fast carbohydrate glucose flux	[mmol/l]
$G_{in_{slow}}(t)$	Slow carbohydrate glucose flux	[mmol/l]
$H_{in_{fast}}$	Cont. transfer function, fast carb.	[-]
$H_{in_{slow}}$	Cont. transfer function, slow carb.	[-]
$H_{sub_{Hum}}$	Cont. transfer function, Humalog	[-]
$I_{sub}(t)$	Total Insulin Absorbtion	[uU/l]
$I_{sub_{Hum}}(t)$	Humalog Insulin Absorbtion	[uU/l]
$I_{sub_{IT}}(t)$	Insulatard Insulin Absorbtion	[uU/l]
$u_{fast}(t)$	Fast Carbohydrate Intake	[g]
$u_{Hum}(t)$	Humalog Injections	[U]
$u_{IT}(t)$	Insulatard Injections	[U]
$u_{slow}(t)$	Slow Carbohydrate Intake	[g]
s	Factor in the Berger model	[-]
T_{50}	Absorbtion halftime	[min]
u_1	Another notation for I_{sub}	[uU/l]
u_2	Another notation for G_{in}	[mmol/l]
V	Sum of squared residuals	$[(mmol/l)^2]$
V	The plasma volume	[l]
$x_{fast}(t)$	State vector of the fast carb. comp. model	[-]
$x_{GIIM}(t)$	State vector of the GIIM used in the PEM-ident.	[-]
$x_{Hum}(t)$	State vector of the Humalog comp. model	[-]
$x_{slow}(t)$	State vector of the slow carb. comp. model	[-]
$y(t)$	Detrended blood glucose concentration	[mmol/l]
$y_{log}(t)$	$y(t)$ transformed by the natural logarithm	[-]
$y_{kov}(t)$	$y(t)$ transformed by the transform proposed by Kovatchev	[-]

List of Abbreviations

Abbreviation	Description
AIC	Akaike Information Criteria
ARX	Auto Regressive with eXternal input
ARMAX	Auto Regressive Moving Average eXternal input
FPE	Final Prediction Error
GIIM	Glucose/Insulin Interaction Model
GSM	Glucose Sub-Model
GTFM	General Transfer Function Model
IDDM	Insulin-Dependant Diabetes Mellitus
IDT	Insulin-Dependant Tissue
IIT	Insulin-Independent Tissue
ISM	Insulin Sub-Model
NARMAX	Non-linear Auto Regressive Moving Average eXternal input
RMS	Root Mean Square
VAF	Variance Accounted For

Contents

Chapter 1

Introduction

1.1 Background

Diabetes Mellitus is a disease characterized by the inability of the pancreas to produce sufficient amounts of insulin. To cover the deficiency 4-6 insulin injections have to be taken daily. The aim of this insulin therapy is to keep the blood glucose level as constant as possible. To determine the amount and timing of these injections different approaches are used. Mostly qualitative and semi-quantitative models and reasoning are used to design such a therapy. In this Master Thesis an attempt is made to show how system identification and automatic control perspectives may be used to estimate quantitative models and to develop insulin therapies. Most patient monitor their blood glucose using personal glucose meters, and determine their own insulin injections based on these results. Poorly controlled blood glucose levels may result in severe complications. Hypoglycemia, low glucose levels, may lead to brain damage[10], coma and eventually death. Hyperglycemia, high blood glucose, on the other hand, can result in chronic damages such as retinopathy, kidney failure and amputation. The purpose of this thesis is to develop a model for predictions based on daily monitoring of blood glucose. Such a model along with an algorithm for the determining of insulin doses, an effective decision support tool can be constructed. This may hopefully facilitate the daily life of diabetes patients and reduce the risks of severe complications.

1.2 The Present

Diabetes therapy research can roughly be divided in two parts: Optimal Insulin regimen control and insulin pump control. The former, which this thesis subjects, is concerned with how to keep blood glucose levels as normal as possible using subcutaneous injections of different insulin types. This is the therapy form primarily used today. The latter, pump therapy, is based

on a insulin pump which continuously feeds the patient with insulin. The insulin pumps used today are pre-programmed to infuse insulin according to a specified scheme. Before meals and exercise a button is pushed, altering the infusions to match the new demands. But the real advantages of a insulin pump is the possibility of a closed-loop controller, acting on the information of the present blood glucose level directly. This is subject to intensive research, and hopefully closed-loop pump control may be the common treatment in a not too distant future. An other way to divide the therapies is of course to make the distinction between open and closed loop control. All current therapies are more or less open loop control. Each patient sets their own insulin regime with aid from their physician based on HbA1c, personal observations and a qualitative estimate of the glucose data. These regimes are to their nature rigid and non-flexible. They form the basis for the therapy and patient often have, and are encouraged to, alter their injection doses when their behavior deviate from the routine the regime was based on. In these situations the patients have to rely on their own knowledge and understanding of the disease to correct their doses. Many patient would benefit from some sort of decision support in these situations. Today none exists.

1.3 Purpose

The purpose of this thesis is to try different modelling approaches on Diabetes Mellitus. These models will be used for prediction of future blood glucose values. To find the best model different validation criteria will be used. Given data on present and previous blood glucose values, the aim is to predict the glycemic behavior for the next two hours with a reasonable accuracy. This accuracy is here defined as a standard deviation of the prediction error less than 0.5 mmol/l.

The models will be estimated and validated using primarily one patient's data. It would be preferable to validate the models using other patients data as well, but due to the scarcity of data this is not possible. This is of course a severe limitation, which has to be regarded seriously when evaluating the validity of the models.

Chapter 2

Physiology

Below a very brief simplified description of the glucoregulatory system will follow. It is intended to give medically novices such as myself a short background to the following thesis. Only the carbohydrate metabolism will be considered.

2.1 The Glucoregulatory System

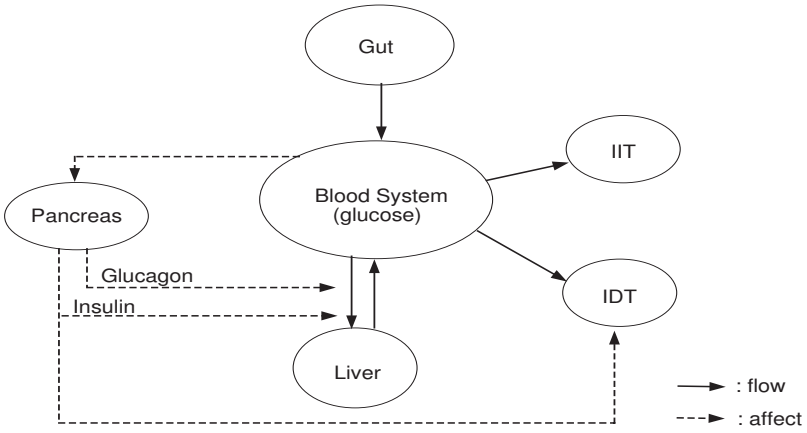

Figure 2.1: Overview of the glucoregulatory system.

The glucoregulatory system is concerned with glucose metabolism and the insulin/glucose mechanisms needed to maintain normoglycemia. In Fig. 2.1 a simplified overview of the flow of glucose and insulin between the most important organs relevant for this system. Below a short description of the these organs and their role in the so called absorbative state and the post absorbative state, the two parts that make up the metabolistic

cycle. A brief description of insulin absorbtion from insulin injections will also be presented. Emphasis will be put on the digestive system and insulin absorbtion from injections.

The absorbative state is the time following a meal during which the ingested carbohydrates are digested and absorbed. During this period excess glucose is absorbed and stored for later use. The postabsorbative state is the time after a meal when the gastro-intestinal tract is empty and energy has to be provided by the body's own storages.

2.1.1 Carbohydrate digestion and absorbtion

Food consists of a number of different nutrients, such as carbohydrates, proteins and fats. Only carbohydrates can primarily be converted into glucose. However, depending on the composition of the meal and the type of carbohydrates the glucose flux from the gut into the blood is altered. There are three main types of carbohydrates; monosaccharides, disaccharides and polysaccharides. Monosaccharides do not have to be split up, but can be absorbed in the blood system directly. Di- and polysaccharides on the other hand have to be split up in a number of steps before they are finally converted to glucose and can be absorbed. Another factor that also alters the absorbtion rate is the composition of the meal. The amount of fats, proteins and fibers contribute in a complex fashion to the digestion dynamics. To describe this phenomenon a concept called Glycemic Index has been introduced. In this thesis this concept will not be used. In fact the composition of meals regarding fat, protein or fiber will not be addressed at all. The only information about the content of the meal that will be used is the quality(mono-,di- or polysaccharide) and quantity(g) of carbohydrates.

The Digestive System

The digestive system consists of the so called gastrointestinal tract and the accessory organs providing the necessary substances for digestion. The gastrointestinal tract is formed by four main parts; mouth, stomach, small intestine and large intestine, all with different functions in the digestive process. Here a short description of these parts and their functions relevant to carbohydrate digestion and absorbtion will follow. Fig. 2.2 provides a good overview of the flow of food through the system.

The digestion starts in the *mouth*. Here the main function is to partly dissolve the macro structure of the food by chewing. The saliva secreted by the salivary glads moistens and lubricates the food particles before swallowing. It also contains the enzyme amylase, which reacts with the polysaccharides, starting the digestion to monosaccharides.

In the *stomach* the last structure of the food is dissolved by the high concentration of hydrochloric acid produced and secreted by specialized stom-

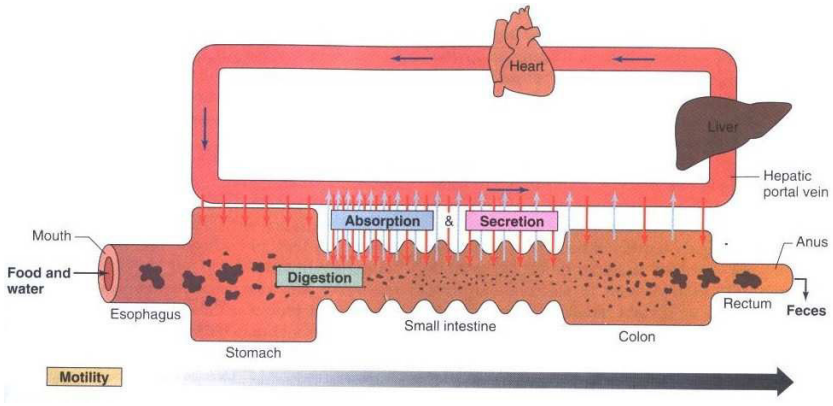

Figure 2.2: Gastrointestinal Tract -Overview[40].

ach wall cells. The amylase in the saliva, swallowed together with the food, continues the digestion of polysaccharides started in the mouth, until the amylase is destroyed by the gastric acid.

The next stage in the process is the *small intestine*. Here the majority of digestion and absorbtion takes place. Bile is secreted by the gallbladder to neutralize the gastric acid from the stomach. Enzymes for digestion are provided by the pancreas. These enzymes react with the poly- and disaccharides, reducing them to monosaccharides. The monosaccharides are thereafter absorbed by transporter-mediated processes into the capillaries and thereby finally reach the portal vein.

All unabsorbed materia is further processed in the *large intestine*. Fiber cannot be digested by the enzymes in the small intestine, but is here metabolized by bacteria. Water and salts are absorbed, solidifying the remnants, called feces.

2.1.2 The Liver

During the absorbative stage glucose is converted and stored as the polysaccharide glycogen. This process is stimulated by insulin. During the post-absorbative stage the glycogen storage is broken down to glucose and released into the blood stream providing energy for the body cells. This process is stimulated by glucagon and inhibited by insulin. Apart from converting glycogen to glucose, new glucose can be formed from protein and fat in the so called glucogeneogenesis. The metabolism of consumed alcohol inhibits this process, which may result in severe hypoglycemia in diabetics.

2.1.3 The Pancreas

In the pancreas two important hormones relevant to the glucoregulatory system are synthesized, namely insulin and glucagon. Insulin release is mainly stimulated by elevated blood glucose concentration. Therefore substantial amounts are released in the absorbative stage, when the glucose level is raised due to the absorbtion from the gut. Glugacon, which has an opposite effect on the liver is accordingly released when blood glucose concentration falls. These two hormones are thus in a feedback arrangement with the blood glucose concentration, controlling the glucose metabolism.

2.1.4 Insulin Dependant Tissue(IDT)

Insulin dependant tissue is dependant on insulin to take up glucose. This mechanism is discussed in the insulin section. Much of the insulin dependant tissue is made up of skeletal muscles. In the absorbative state, skeletal muscle cells not only consume the glucose directly, but also converts some to glycogen providing a energy storage for later use.

2.1.5 Insulin Independent Tissue(IIT)

Insulin independent tissue such as the brain and the central nervous system do not need insulin to utilize glucose.

2.1.6 Insulin

Insulin is the major hormone controlling glucose metabolism. It is a protein consisting of three peptide parts; a A-, B- and C-chain. In healthy subjects it is produced in the beta-cells in the pancreas whereas diabetics depend mostly on artificially produced insulin analogs. Previously animal insulin has been used, but due to, among other things, development of insulin antibodies in patients treated with these insulins, most insulin is today produced using bacterial or yeast processes[39]. All insulins, artificial or not, will hereafter be referred to as simply insulins.

Insulin Absorbtion

Insulin is injected subcutaneously in a number of different spots. Rapid acting insulin is injected in the abdominal fat layer, whereas long-lasting insulin is usually taken in the upper side of the thigh. From these depots the insulin is transferred to the blood system via the capillaries. The absorbtion rate depends on a series of factors[25]. One contributing factor is the capillary density. A higher density results in a greater diffusion area between the depots and the capillaries. The abdominal region has the highest capillary density and the thigh the lowest[25]. This explains why rapid acting

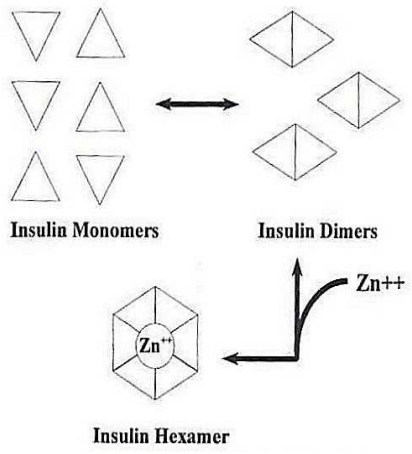

Figure 2.3: Molecular structure of insulin[13].

insulin is preferably infused in the stomach and long-lasting in the thigh. The size of the insulin molecules is a dominant rate limiter. Large molecules will have difficulties passing through the capillary pores. The structure of the insulin molecules are either monomer, dimer or hexamer. Insulin will spontaneously form hexamers if the concentration is sufficiently high. This so called self-association can be catalyzed by zinc ions. Therefore zinc is added to the insulin solution in slow acting insulins, thereby considerably reducing the absorbtion rate[25]. In the rapid acting insulins the insulin molecules are mainly monomeric or dimeric. They have been modified so that hexamer formation is avoided altogether[39]. Therefore they are also called monomeric insulins. Another major factor affecting the absorbtion rate is the size of the injection dose. A large dose reduces the ratio between the absorbtion area and the depot volume, thus reducing the absorbtion. A number of studies have been undertaken, all indicating a linear relationship between insulin dose and absorbtion halftime[8, 4] as can be seen in Fig. 2.4.

These studies have been undertaken on slow acting or intermediate acting insulins. However, recent studies indicate both theoretically and experimentally that the linear relationship is not valid for monomeric insulin[11]. Finally, blood flow and temperature of the injected site have a significant contribution to absorbtion rate. Raised temperature enhances the disassociation of hexameric insulin and accelerates insulin diffusion. Increased blood flow raises absorbtion rate. Thus exercise plays a key role for absorbtion, since it raises both body temperature and blood flow.

After the absorbtion from the depots the insulin is circulated in the blood system and finally interacts with a insulin receptor at the cell surface.

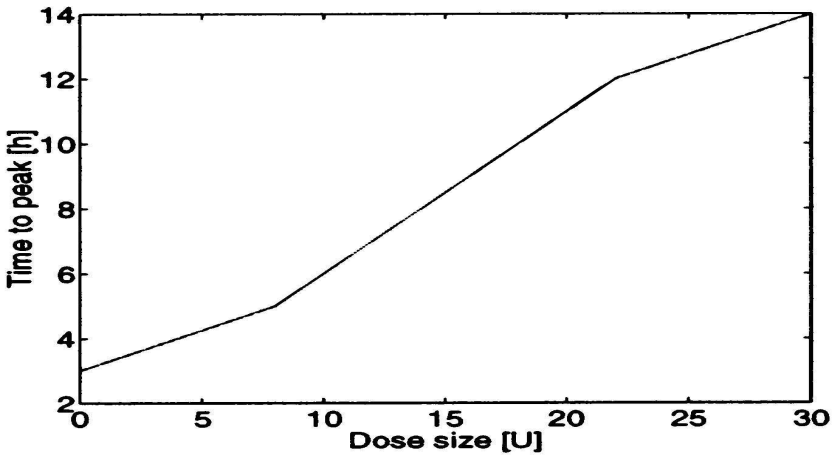

Figure 2.4: Dose-dependant Absorbtion Time[4].

Insulin Receptors

The insulin receptors are so called tetramers consisting of two α- and two β-subunits. The α-subunits are entirely extracellular and serves as a binding site for the insulin molecule. When the insulin has attached to the α-subunits a signal process is initiated via the β-subunits, resulting in increased glucose transporter activity. The glucose transporters facilitate glucose cell membrane crossing, thereby reducing blood glucose concentration. The receptor/transporter cycle can be seen in Fig. 2.5. There are different types of glucose transporters and, so far, five different types have been found[41]. Not all of these types require insulin to become active. Therefore the glucose utilization is divided into insulin dependant and insulin independent utilization.

It is a well known fact that exercise enhances insulin sensitivity and is therefore one part of common Type 2 therapy. What actually causes the increased insulin sensitivity is however still not well understood. Studies indicate that the GLUT4 transporter activity is stimulated, thus resulting in increased insulin dependant glucose utilization[29].

Insulin Therapy

Type 1 diabetics are treated with a therapy called basal/bolus regime. The intention is to mimic the normal behavior in a healthy person. The basal injection is a slow-acting insulin taken once or twice a day. It serves to preserve a basal level of insulin required to maintain normal activity. The basal injections are rapid acting insulin injections taken to counteract the massive glucose flux following a meal. The slow-acting insulin used here is Insulatard and the rapid-acting insulin is Humalog.

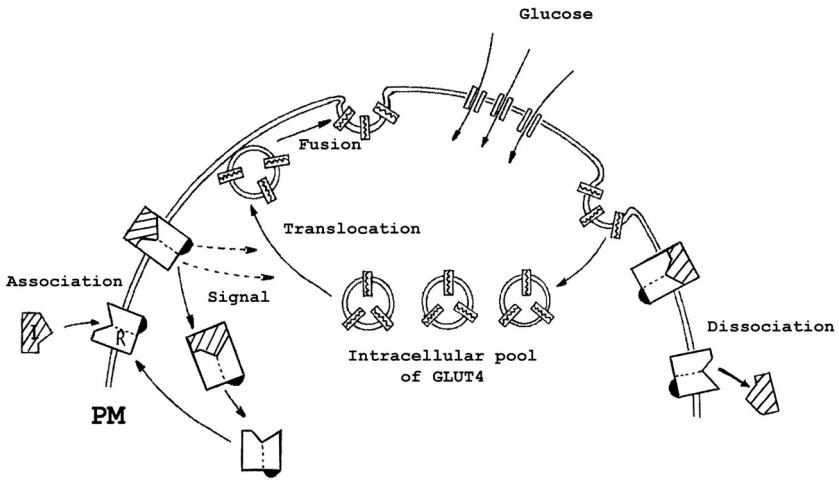

Figure 2.5: Insulin Receptor and Glucose Transporter Cycle[38].

Insulatard

Insulatard is an intermediate/long-lasting insulin of NPH-type. The approximate time action profile provided by the manufacturer can be seen in Fig. 2.6.

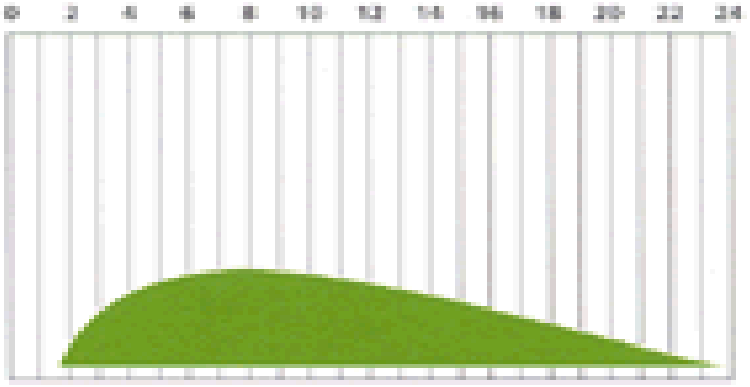

Figure 2.6: Time action profile of Insulatard[2].

Humalog

Humalog is rapid action monomeric insulin. According to the manufacturer the time action profile looks like this:

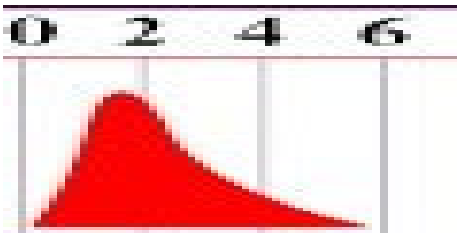

Figure 2.7: Time action profile of Humalog[1].

2.2 Insulin Dependant Diabetes Mellitus(IDDM)

In Insulin Dependant Diabetes Mellitus, or as it also is called Diabetes Type 1, the insulin production is completely or severely reduced. This is due to the destruction of the insulin-producing β-cells in the pancreas by the body's own immune system. To cover the loss, several insulin injections have to be taken daily.

Unregulated or poorly regulated IDDM leads to constant hyperglycemia, high blood glucose concentration. This state can have serious both short term and long term consequences. Severe hyperglycemia can result in coma and death, as a result of ketoacidosis or severe dehydration. The later is the result of that the renal function of reabsorbing glucose is saturated, which also has the effect that large quantities of water is also extracted together with the glucose, by the so called osmatic diuresis phenomenon.

Hypoglycemia, low blood glucose concentration, may be the result of for example too large doses of insulin or physical activity without reduced insulin doses. Hypoglycemia has most consequences for the brain, which is almost entirely dependant on glucose as fuel. The symptoms range from headache, confusion and aggressive behavior to coma and finally death depending on the severity of the hypoglycemia.

2.2.1 The Honey-moon Period

After the diagnosis of IDDM a period of shifting disease patterns follow. This is the result of the β-cells recovering somewhat, when the insulin, coming from the insulin injections, assist them. This period lasts a couple of months.

2.2.2 Dawn phenomenon

There is evidence that the insulin sensitivity is reduced in the morning. This is called the dawn phenomenon.

2.3 Partitioning the System

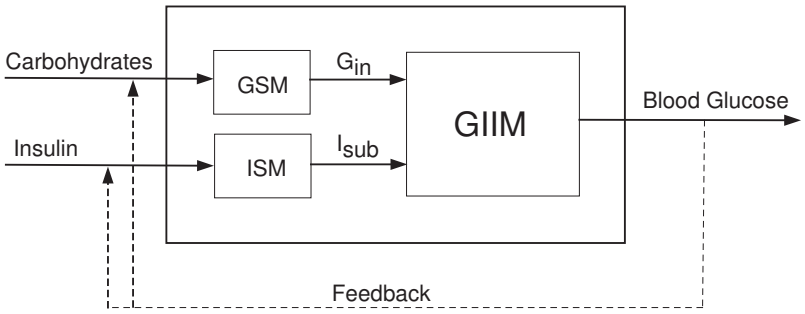

Figure 2.8: The partitioning of the system.

For modelling purposes the system will be considered to consist of three main parts; the Glucose Sub-Model(GSM), the Insulin Sub-Model(ISM) and the Glucose/Insulin interaction Model(GIIM). The GSM describes the absorbtion of glucose from meal, the ISM the absorbtion of insulin from insulin injections and the GIIM the interaction of glucose and insulin in the blood system and organs. These three parts will be modelled separately using mainly compartment models and linear black-box models.

Chapter 3

Methods

In this chapter a brief description of the methods used in this thesis will be presented. For explanation of terms used, and a more thorough description of the methods, please refer to the references.

3.1 Linear Regression[28, 33]

The general linear regression model is:

$$y(k) = \varphi(k)^T \cdot \theta + e(k) \tag{3.1}$$

where y(k) is the variable of interest, θ is the parameter vector and $\varphi(k)$ is the so called regression vector. To estimate the parameters the following data matrices are formed:

$$\mathcal{Y}_N = \begin{pmatrix} y(1) \\ y(2) \\ \vdots \\ y(N) \end{pmatrix}, \Phi_N = \begin{pmatrix} \varphi(1)^T \\ \varphi(2)^T \\ \vdots \\ \varphi(N)^T \end{pmatrix} \tag{3.2}$$

The least squares criteria is to minimize the sum of the squared errors between the model and the observations:

$$V(\theta) = \frac{1}{2} \cdot (\mathcal{Y}_N - \Phi_N\theta)^T \cdot (\mathcal{Y}_N - \Phi_N\theta) \tag{3.3}$$

Minimize w.r.t θ:

$$\frac{\partial V(\theta)}{\partial \theta} = -\mathcal{Y}_N^T \cdot \Phi_N + \theta^T \cdot (\Phi_N^T \Phi_N) = 0 \tag{3.4}$$

The minimum is obtained for:

$$\hat{\theta} = (\Phi_N^T \Phi_N)^{-1} \Phi_N^T \mathcal{Y}_N \tag{3.5}$$

3.1.1 Recursive Least Squares Estimation

For time-varying systems the parameters have to be updated as they change. This is done using the recursive least squares estimation routine with exponential forgetting:

$$\hat{\theta}(t) = \hat{\theta}(t-1) + K(t)(y(t) - \varphi^T \hat{\theta}(t-1)) \tag{3.6}$$
$$K(t) = P(t)\varphi(t) \tag{3.7}$$
$$P(t) = (I - K(t)\varphi^T)P(t-1)/\lambda \tag{3.8}$$

where $P(t)$ is an estimate of the covariance matrix of the parameters at time t and λ is the so called forgetting factor determining how fast the parameters can be changed. $P(0)$ is often set to a unit matrix multiplied with i.e. 1000, to allow a fast approach to the correct initial parameter values. The best value of the forgetting factor,λ has to be found by trial and error if no prior knowledge is available.

3.2 ARMAX Models[28, 33]

The ARMAX models all have the following structure:

$$A(z^{-1})y(k) = z^{-k_1}B_1(z^{-1})u_1(k) + \ldots + z^{-k_n}B_n(z^{-1})u_n(k) + C(z^{-1})\omega(k) \tag{3.9}$$

where y(k) is the output of interest,$u_1 \ldots u_n$ are the inputs and $k_1 \ldots k_n$ are the time delays for each input. The polynomials $A(z^{-1}), B_i(z^{-1})$ and $C(z^{-1})$ are:

$$A(z^{-1}) = 1 + a_1 z^{-1} + \ldots + a_{n_A} z^{-n_A} \tag{3.10}$$
$$B_i(z^{-1}) = b_{0,i} + b_{1,i} z^{-1} + b_{n_{B_i},i} z^{-n_{B_i}} \tag{3.11}$$
$$C(z^{-1}) = 1 + c_1 z^{-1} + \ldots + c_{n_C} z^{-n_C} \tag{3.12}$$

Thus the parameter vector is:

$$\theta = \begin{pmatrix} a_1 \ldots a_{n_A} & b_{0,1} \ldots b_{n_{B_1},1} \ldots b_{0,l} \ldots b_{n_{B_l},l} & c_1 \ldots c_{n_C} & \sigma_\omega^2 \end{pmatrix} \tag{3.13}$$

3.3 Subspace Models[28, 23]

The subspace approach differs from the previous in that instead of looking at the transfer function of the system the state space equations are considered:

$$x(k+1) = Ax(k) + Bu(k) + \omega(k) \tag{3.14}$$
$$y(k) = Cx(k) + Du(k) + \upsilon(k) \tag{3.15}$$

This system is equivalent to the innovations model:

$$x(k+1) = Ax(k) + Bu(k) + Ke(k) \tag{3.16}$$
$$y(k) = Cx(k) + Du(k) + e(k) \tag{3.17}$$

The following relation holds if no noise is considered:

$$\begin{pmatrix} y(0) & \dots & y(N-1) \\ \vdots & \ddots & \vdots \\ y(i-1) & & y(N+i-2) \end{pmatrix} = \begin{pmatrix} C \\ CA \\ \vdots \\ CA^{i-1} \end{pmatrix} \cdot \begin{pmatrix} x(0) & \dots & x(N-1) \end{pmatrix} + \\ + \begin{pmatrix} D & 0 & \dots & 0 \\ CD & D & & \\ \vdots & & & \\ CA^{i-2}B & CA^{i-3}B & \dots & D \end{pmatrix} \cdot \begin{pmatrix} u(0) & u(1) & \dots & u(N-1) \\ u(1) & u(2) & & u(N) \\ \vdots & & \ddots & \\ u(i-1) & & & u(N+i-2) \end{pmatrix} \tag{3.18}$$

Using a more compact notation:

$$Y_{i,N} = \Gamma_i X_N + H_i U_{i,N} \tag{3.19}$$

Now modelling the noise properties as well calls for two more terms:

$$Y_{i,N} = \Gamma_i X_N + H_i U_{i,N} + G_i W_{i,N} + V_{i,N} \tag{3.20}$$

The matrix G_i looks like this:

$$G_i = \begin{pmatrix} 0 & 0 & \dots & 0 \\ C & 0 & & \\ CA & C & \ddots & \\ \vdots & & & \\ CA^{i-2} & CA^{i-3} & \dots & 0 \end{pmatrix} \tag{3.21}$$

while $W_{i,N}$ and $V_{i,N}$ are the Hankel matrices of $\upsilon(k)$ and $\omega(k)$.

Given $Y_{i,N}$ and $U_{i,N}$ the B,D, K and x_0 can be estimated using singular value decomposition following the PO-MOESP-algorithm. For details see [23].

3.4 Kalman Filter[28, 5]

Consider the state space model:

$$x(k+1) = \Phi x(k) + \Gamma u(k) + \upsilon(k) \tag{3.22}$$
$$y(k) = Cx(k) + Du(k) + e(k) \tag{3.23}$$

with $E(\upsilon(k)) = 0$ and $E(e(k)) = 0$ and

$$E(\upsilon\upsilon^T) = R_1 \tag{3.24}$$
$$E(ee^T) = R_2 \tag{3.25}$$
$$P((0) = E(x(0)x(0)^T) = R_0 \tag{3.26}$$

Then the states can be predicted by:

$$\hat{x}(k+1) = \Phi\hat{x}(k) + \Gamma u(k) + K(k)(y(k) - C\hat{x}(k)) \tag{3.27}$$

where

$$K(k) = \Phi P(k)C^T(R_2 + CP(k)C^T)^{-1} \tag{3.28}$$
$$P(k+1) = \Phi P(k)\Phi^T + R_1 - \Phi P(k)C^T(R_2 + CP(k)C^T)^{-1}CP(k)\Phi^T \tag{3.29}$$

3.5 Compartment Models[19]

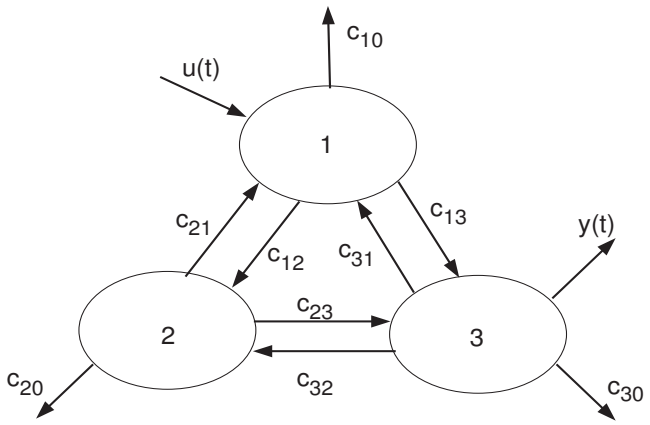

Figure 3.1: Three-compartment model.

A compartment model is a model where the structure of the system is postulated, a so called grey-box model. The system is divided into separate entities, called compartments. Between these compartments energy and material flow with different rate constants, c_{ij}. In Fig. 3.1 a three-compartment model is sketched. This will serve as an example of how a compartment model works. The system equations are:

$$\dot{x} = \begin{pmatrix} -\sum_{i\neq 1}^{3} c_{1i} & c_{21} & c_{31} \\ c_{12} & -\sum_{i\neq 2}^{3} c_{2i} & c_{32} \\ c_{13} & c_{23} & -\sum_{i\neq 3}^{3} c_{3i} \end{pmatrix} x + \begin{pmatrix} 1 \\ 0 \\ 0 \end{pmatrix} u(t) \tag{3.30}$$

$$y(t) = \begin{pmatrix} 0 & 0 & 1 \end{pmatrix} x(t) \tag{3.31}$$

3.6 Model Validation[28]

A number of criteria are used to decide which the best model is, given a set of different models.

3.6.1 Loss Function

The loss function is the simplest criteria to evaluate the model's accuracy.

$$V = \frac{1}{2} \cdot (\mathcal{Y}_N - \hat{\mathcal{Y}}_N)^T \cdot (\mathcal{Y}_N - \hat{\mathcal{Y}}_N) \tag{3.32}$$

3.6.2 Akaike Cost Criteria(AIC)

The loss function do not take the model's complexity into consideration. There is a point in penalizing large models to avoid over-parametrization. This can be done by the AIC:

$$AIC = \log(V) + \frac{2p}{N} \tag{3.33}$$

where p is the number of parameters and N the length of the data vector.

3.6.3 Final Prediction Error(FPE)

The AIC has been found to overestimate the number of parameters motivating alternative criteria. One such is the FPE:

$$FPE = \frac{2}{N} \cdot \frac{N+p}{N-p} \cdot V \tag{3.34}$$

3.6.4 Variance Accounted For(VAF)

Once a model has been selected next is to evaluate the performance of the model. One way to get a quantitative measure of this is the VAF:

$$VAF = (1 - \frac{(\mathcal{Y}_N - \hat{\mathcal{Y}}_N)^T(\mathcal{Y}_N - \hat{\mathcal{Y}}_N)}{\mathcal{Y}_N^T \hat{\mathcal{Y}}_N}) \cdot 100 \tag{3.35}$$

3.6.5 Root Mean Square Error(RMS)

Another measure to evaluate the similarity between two signals is the RMS:

$$RMS = \sqrt{\frac{\sum_{k=1}^{N}(y_k - \hat{y}_k)}{N}} \tag{3.36}$$

Chapter 4

Data

4.1 Blood Glucose

4.1.1 Data Collection

The data primarily used in this thesis was collected during the first six months of a newly diagnosed type 1 patient. The glucose testing was undertaken using a personal blood glucose tester, Accu-check Compact, Roche Diagnostics. Meals, insulin injections and glucose samples were noted and registered in a dairy. In Fig. 4.1 a typical day can be seen, with the scheduled samplings as well as some unscheduled samplings.

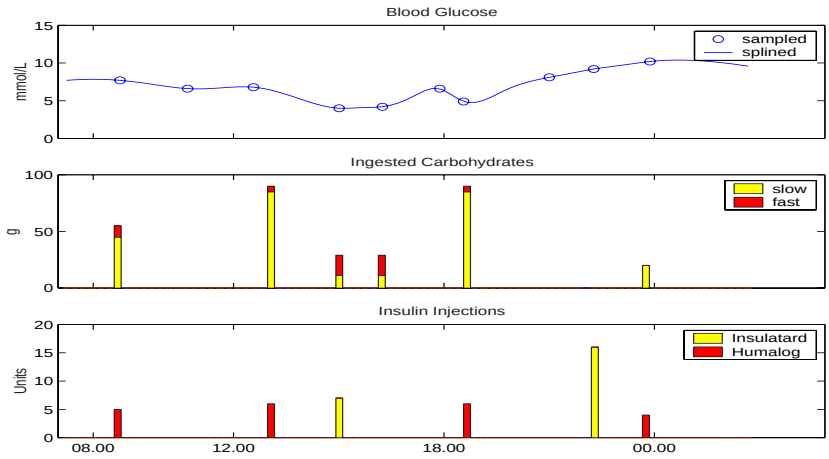

Figure 4.1: A typical day.

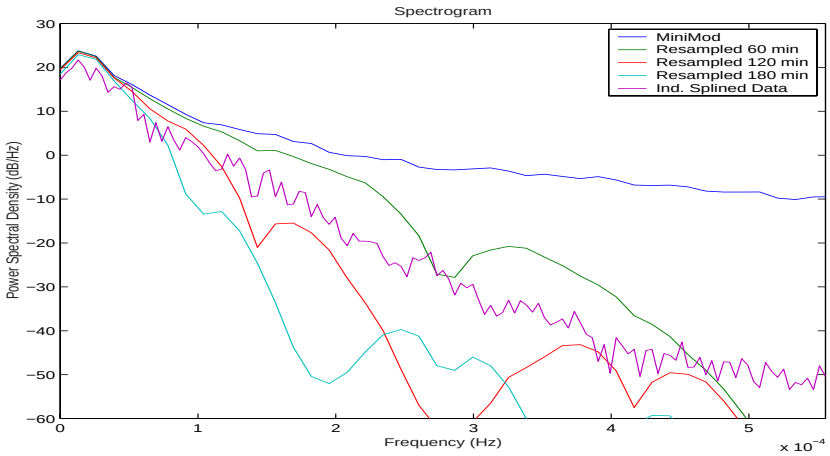

Figure 4.2: Comparison between the spectrograms of MiniMod data, resampled and interpolated MiniMod data and interpolated home-monitored data.

4.1.2 Sampling Frequency

The glucose sampling was based on a sampling schedule following the daily routine. To capture the rapid dynamics caused by the intake of carbohydrates, samples were taken before and 1.5 hours after each meal. Sampling was also scheduled at the late Insulatard injection. Additional to these measurements further unscheduled samples were collected, making the average sampling frequency 9.3 samples/day. Is this sufficient to capture the dynamics of the underlying physiological system? According to Shannon's sampling theorem:

$$f_s \geq 2f_{max} \tag{4.1}$$

where f_{max} is the highest frequency of interest. According to [43] at least 8 samples per day are needed to get the lowest essential dynamics of the system, namely the rise and fall of the blood glucose level due to the carbohydrate intake. This relies on the assumption that the meal related period is about 6 hours. This assumption is supported by the periodic behavior of the blood glucose change plotted in Fig. 4.10. So sampling every third hour is needed to capture the basic meal related dynamics, but what sampling frequency is needed to reconstruct the blood glucose curve reliably? To find the highest frequency of interest records of 56 patients monitored by MiniMed were analyzed[1]. This data was sampled at 5 min intervals, well below the fastest dynamics of the system. The data was resampled at a lower rate and splined using the reconstructing method used for the home-monitored data. In Fig. 4.2 the spectrogram of the average MiniMod measurements

[1]Provided by Novo Nordisk

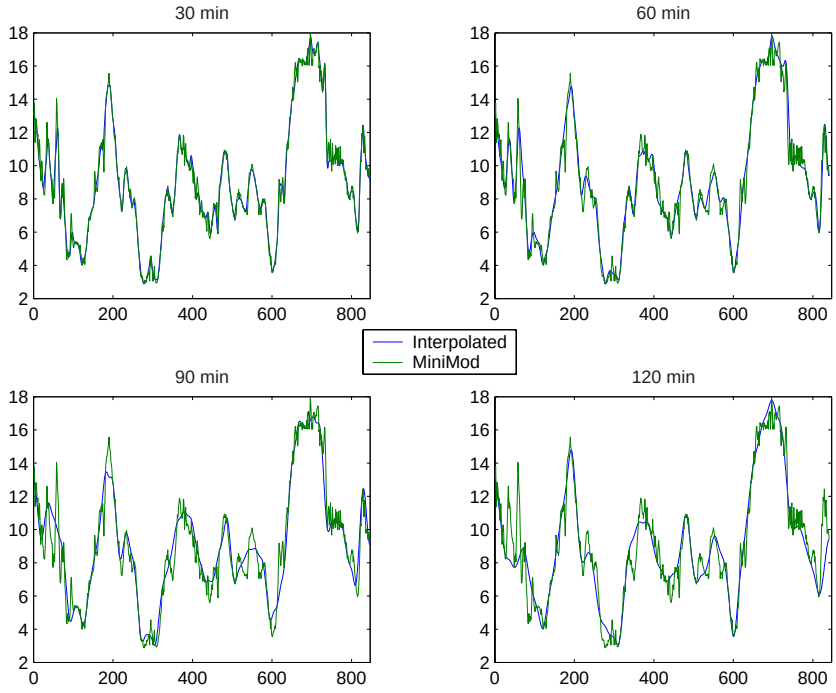

Figure 4.3: Comparison between the reconstructed data and the original data for some different resampling frequencies.

together with the spectrograms of the resampled and interpolated MiniMod data and the spectrogram of the interpolated curve for the home monitored data. The interpolated home monitored data seems to have a similar spectral composition as the 120 min resampled MiniMod data, at least for the lower frequencies. The interesting question is: Does these measurements contain sufficient information to make a reconstruction of the original signal possible? And if so, is the proposed method of interpolation an efficient and reliable way to do so?

The MiniMod data was resampled at a number of lower frequencies than the original and interpolated using the spline method used for the home-monitored data. In Fig. 4.3 a comparison between the original MiniMod data the resampled and interpolated data of a representative patient can be seen. The patient data used here for visualization of the correspondence between the resampled, interpolated data and the original data incorporate some typical and important features of blood glucose data. Rapid and large fluctuations within the normal range of a diabetic makes it suitable as a reference.

In the upper plots the data has been resampled to a sampling interval of 30 min and 60 min. The interpolated curves follow the MiniMod data

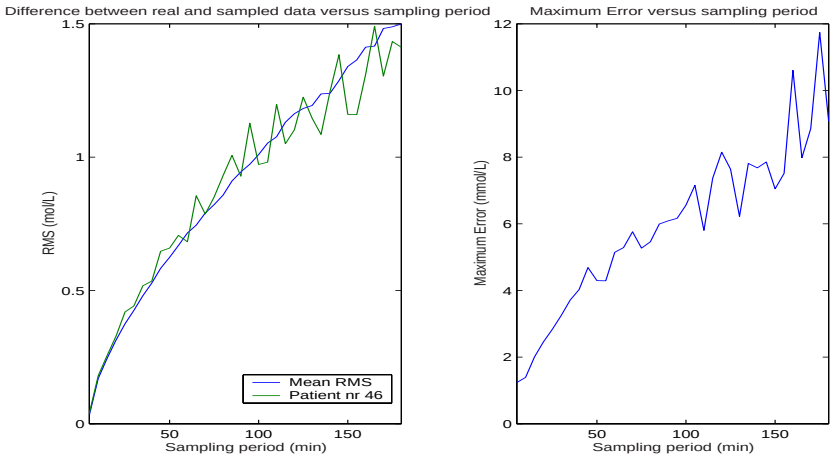

Figure 4.4: RMS of the reconstructed resampled data(left) and maximum error(right) compared to original data.

without complications, smoothing the noisy original. In the lower plots the interpolated curves have more trouble keeping up with the original. The rapid oscillations at the start are missed altogether, the tops and bottoms are not filled out correctly and here and there smaller, more rapid variations are ignored. However, most of the larger variations are present in the interpolation and the total impression is that the splined curves follow the original quite well, but for some few quick ups and downs. This viewpoint is also backed up by the mean root mean square(RMS) between the original signal and the splines seen in Fig. 4.4. The RMS is quite reasonable over the entire range. Looking at the maximum error in Fig. 4.4 gives another impression. This plot shows the worst case for every sampling rate. The low RMS and the high maximum error indicates that some few rapid changes in the blood glucose of large magnitude are not correctly manifested in the interpolated curve. However, glucose self-monitoring does not follow a strict sampling schedule. Rapid changes in the blood glucose are often experienced as hypoglycemia, changes into hypoglycemia or hyperglycemia are often recognized and these circumstances calls for unscheduled measurement to establish glycemic status. Therefore this problem is somewhat self-regulated in a diabetic subject. Assuming that 8 hours is spent sleeping a day, the average sampling period becomes about 100 min. Therefore the interpolated data can perhaps be regarded as having a data reconstruction potential close to the 90min resampled data. This signal misses some of the fast oscillations, but can still be considered to make good estimates of the original data.

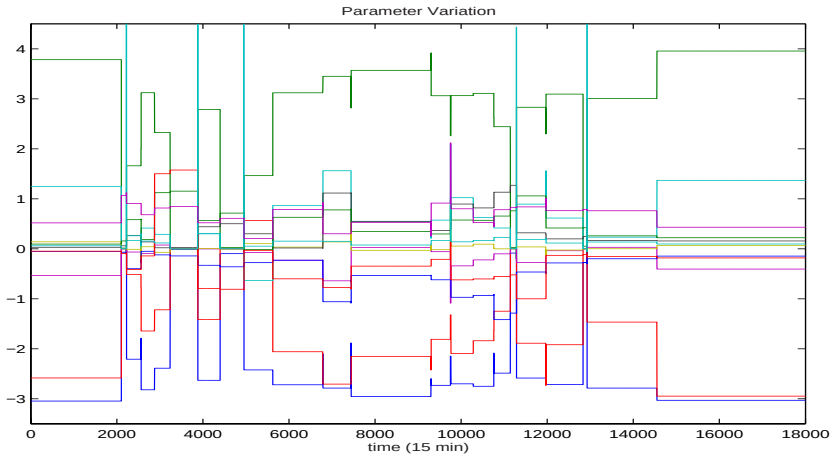

Figure 4.5: Data segmentation using "SEGMENT".

4.1.3 Data Segmentation

The data is collected in the so called honey-moon period during which the pancreatic β-cells recovers somewhat, resulting in considerably varying insulin doses and glycemic response. Mathematically this translates into varying model parameters. In order to estimate and validate different models, data segments with constant parameter values are needed. To find such segments the data was investigated using the Matlab command "segment", a recursive linear model of ARMAX-type. In Fig. 4.5 the parameter variations over the time period can be seen. A number of more steady segments

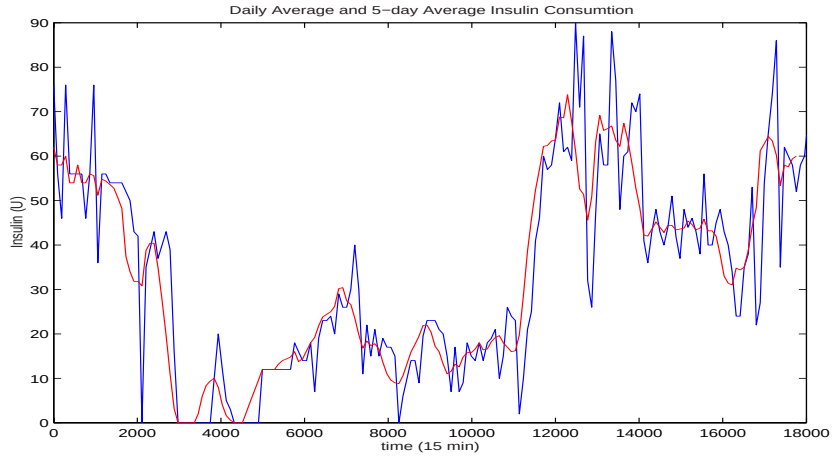

Figure 4.6: Average Insulin Consumption.

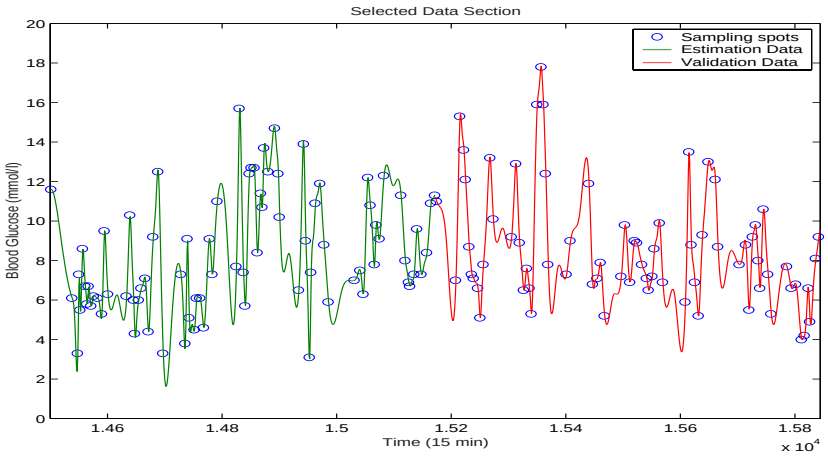

Figure 4.7: The selected data period.

can be identified. Of these the last segment is the most interesting because of a number of factors. Firstly, the patient has had the disease long enough to make up his own regimen, making insulin inputs more varying thereby increasing the excitation from this signal. Secondly, enough time has elapsed since diagnosis to make it plausible that the honey-moon period is over. Thirdly, the daily sum of insulin doses is most even for this period as can be seen in Fig. 4.6, indicating as well that the dynamics are more steady.

From this data segment a smaller segment was extracted corresponding to two weeks of data. The first week will be used for parameter estimation and the second week for validation. In Fig. 4.7 the selected period can be seen.

4.1.4 Measurement Noise

According to typical test series the reproducibility of this tester has a coefficient of variance of 1.7 %[18]. With an average of 8.25 mmol/l for the series this corresponds to a standard deviation of 0.14 mmol/l.

4.2 Carbohydrates

Intake of food was noted semi-quantitatively using predefined meals[2]. Each meal was quantified using three levels; small, normal and large.

Example:

[2]See Appendix A

Time	Food	Type
08.45	Breakfast	Normal
12.30	Lunch	Large
16.00	Snack	Small
18.15	Dinner	Normal

The predefined meals were determined by estimating the composition and size of some standard meals, using [32] and a balance. Carbohydrate content was the only quantity of interest since it is the only ingredient that can be converted to glucose directly. The carbohydrates were divided into two different main types; fast and slow. Mono- and disaccharides were considered fast carbohydrates and the rest were considered slow.

All meals are considered to be ingested within 15 minutes. Thereby the carbohydrate intake can be mathematically expressed as:

Slow Carbohydrate Intake:

$$u_{slow}(t) = \sum_k C_{slow,k} \cdot \delta(t - t_k) \tag{4.2}$$

Fast Carbohydrate Intake:

$$u_{fast}(t) = \sum_k C_{fast,k} \cdot \delta(t - t_k) \tag{4.3}$$

where $C_{slow,k}$ and $C_{fast,k}$ are the amounts(g) of slow and fast carbohydrates ingested at time t_k.

4.3 Insulin

The timing and dose size of each injection was noted. The injections are considered to take place instantaneously:

Insulatard Injections:

$$u_{IT}(t) = \sum_k D_{IT,k} \cdot \delta(t - t_k) \tag{4.4}$$

and Humalog Injections:

$$u_{Hum}(t) = \sum_k D_{Hum,k} \cdot \delta(t - t_k) \tag{4.5}$$

where $D_{IT,k}$ and $D_{Hum,k}$ are the Insulatard and Humalog doses(U) at time t_k.

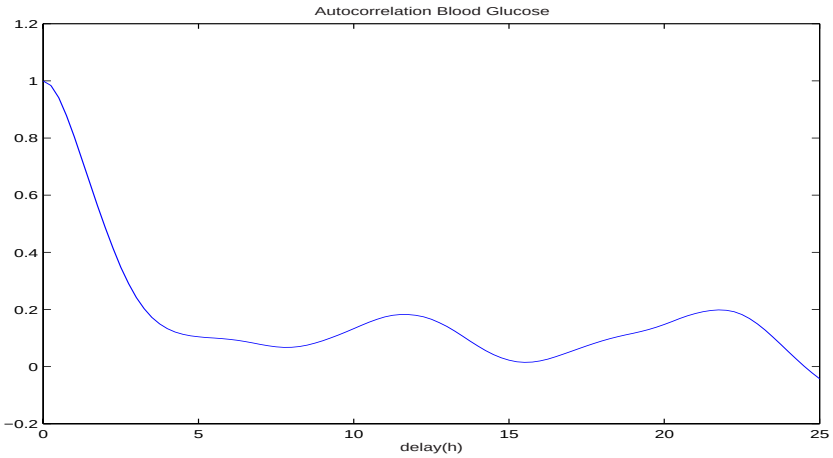

Figure 4.8: Autocorrelation Blood Glucose.

4.4 Data Preprocessing

4.4.1 Detrending

The glucose data was reduced by the average over the two weeks.

4.4.2 Outliers

No obvious outliers could be identified.

4.4.3 Splining

The data was scarce and infrequently sampled. The identification methods used here require uniformed samples. To fulfill this demand the data was interpolated using splines. To avoid under- and overshoots caused by the splines linearly interpolated help spots were added to the original data, a concept used in [7] as well. In order for these spots not to influence the spline in a negative way, different weights were assigned the true data and the help spots during the spline interpolation. The time frame to use was chosen to the 15 min intervals. The reason for this was mainly to use the accuracy concerning the timing of meal intake and insulin injections noted in the diary.

4.5 Statistical Analysis

Here we will consider the statistical properties of the data. Thereby interesting properties of the system can be retrieved. In Fig. 4.8 the autocorrelation

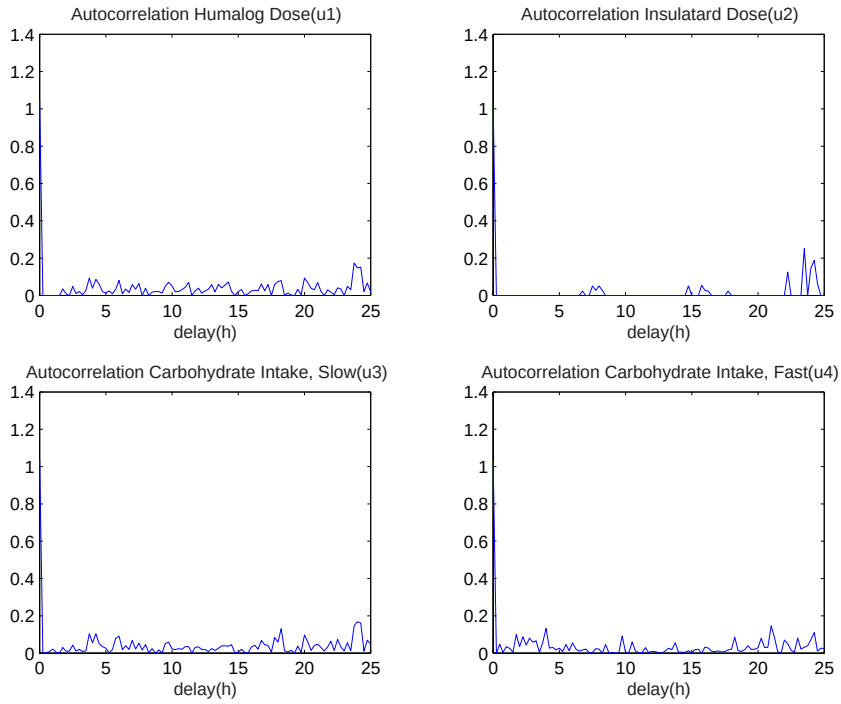

Figure 4.9: Autocorrelation Input Signals.

of the output can be seen. Clearly the data is strongly periodic. This tendency can also be noted by looking at the autocorrelation for the inputs in Fig. 4.9. The insulin doses and the slow carbohydrate intake have a 24-

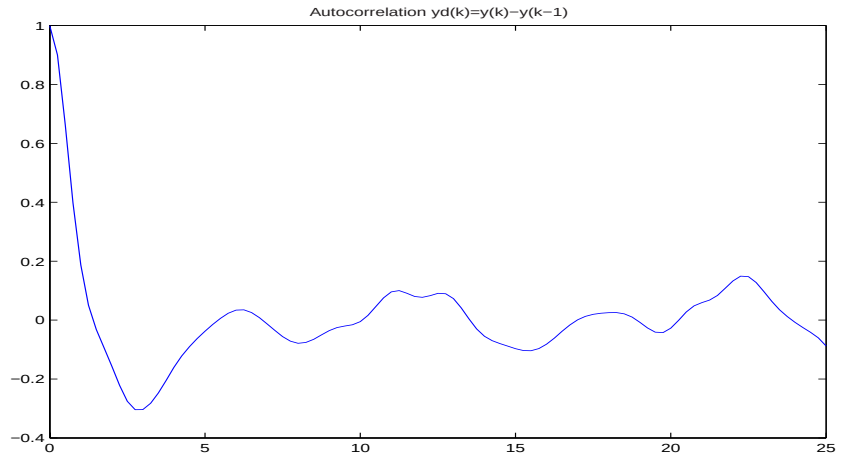

Figure 4.10: Autocorrelation Blood Glucose Change.

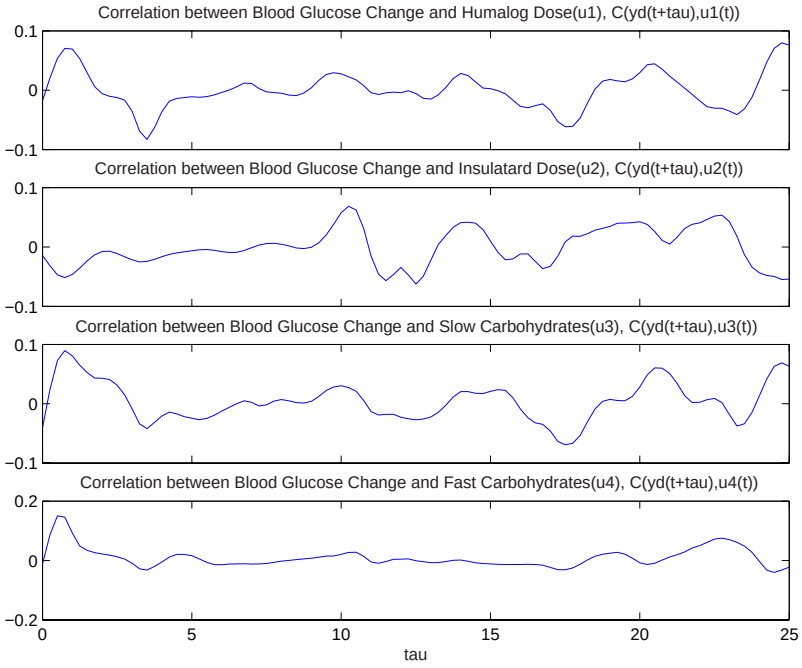

Figure 4.11: Impulse Response Estimates.

hour distinct period. The fast carbohydrates however do not show such a clear periodic behavior, probably due to many snacks at irregular hours. In Fig. 4.10 the autocorrelation of the blood glucose change can be seen. Here the 5-6 hour periodicity of the glucose flux following a meal referred to by Worthington is quite obvious.

In Fig. 4.11 the impulse response estimates(IRE) of the different inputs to the blood glucose change can be seen. These plots highlights one of the major problems in identifying this system under these circumstances, inputs act simultaneously and with opposite effect on the output. Look at the first plot, the impulse response estimate of the rapid-acting insulin. Insulin has a blood glucose lowering effect and thus the IRE ought to be negative. Instead the response is initially positive. This is due to that the rapid-acting insulin almost always is injected when food is ingested. Thus the first positive correlation is the effect of the carbohydrates. After some time the insulin gains the upper hand explaining the negative correlation after about three hours. In the same way the IRE's of the carbohydrates are distorted. This is a serious difficulty obscuring the identification of the system.

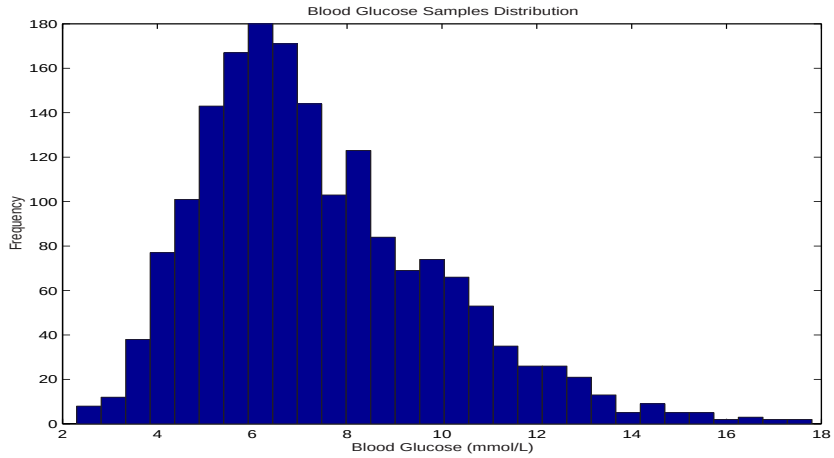

Figure 4.12: Distribution, Blood Glucose Samples.

4.5.1 Log-Normality

The glucose measurements are not normally distributed. The samples fluctuate around an average of about 6-8 mmol/l, but the deviations are not normally scattered around this mean as can be seen in Fig. 4.12. This phenomenon has been noted in [14] as well. In Fig. 4.13 the natural logarithm of the data has been plotted on a so called normal paper. The data is following the normal curve quite well. Another test of normality is the Bera-Jarque test. The normality hypothesis was not rejected($p < 0.01$). Thus is seems reasonable to say that the measurements are log-normally distributed.

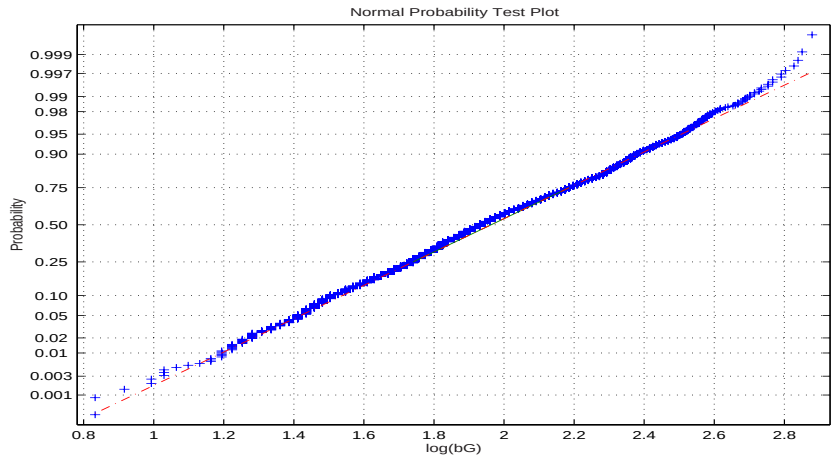

Figure 4.13: Test of log-normality.

Chapter 5

Modelling and Estimating the Sub-Models

In this chapter the insulin absorbtion from insulin injections and the digestive system will be modelled and estimated. First the mathematical models are developed and then these models are estimated using the measured data.

5.1 Modelling the Sub-Models

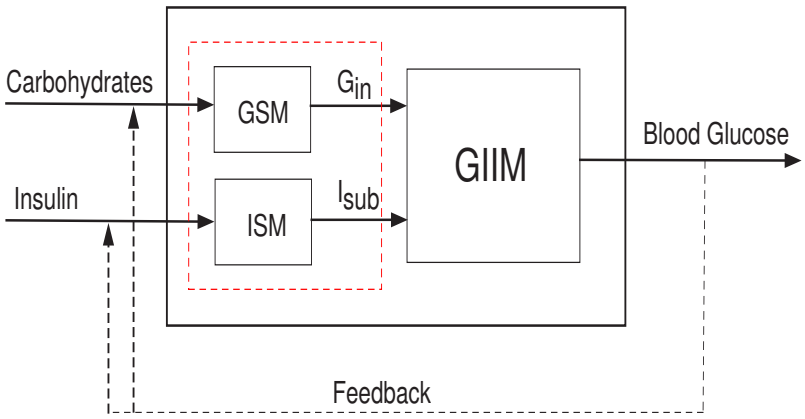

Figure 5.1: Partitioning of the system.

5.1.1 The Insulin Subsystem

Insulin injections form the basis for conventional type 1 therapy. The dynamics of insulin is one of the most important factors affecting the outfall

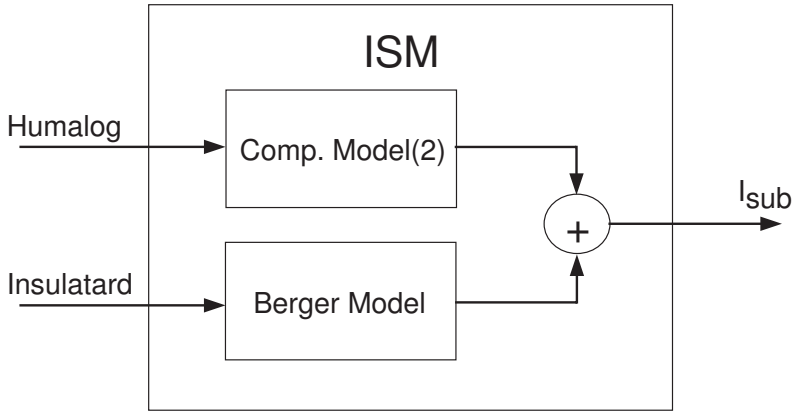

Figure 5.2: The Insulin Sub-Model(ISM).

of the therapy. Much research is targeted at developing new insulin analogs, both long-lasting and rapid-acting ones. However, the mathematical modelling of the insulin action is still quite poorly developed. Most models are either compartment models or highly sophisticated non-linear physiological models[36, 22]. The compartment models are linear and thereby do not include the important non-linearity of dose size dependant dynamics. The non-linear models, on the other hand, are often too complex to be feasible for routinely use. However, there is one model that has been proposed, that both enhances the simplicity of the compartment models as well as featuring the important non-linearity of dose dependant dynamics. It is the model proposed by Berger and Rodbard[8]. It will be used here to represent insulin absorbtion of the slow-acting insulin. As previously has been mentioned, the linear relationship between peak time and insulin dose size does not exist for rapid acting insulin. Glucose clamp studies show that the absorbtion rate is independent of insulin dose size in the range 0.05 to 0.4 U/kg[11] for these insulins. Therefore these injections will be modelled using a classical compartment model. Together the long-lasting and rapid-acting insulin absorbtions form the total insulin flux:

$$I_{sub}(t) = I_{sub_{IT}}(t) + I_{sub_{Hum}}(t) \tag{5.1}$$

Below a brief description of the modelling of the two insulins will follow.

Insulatard, $\mathbf{I_{sub_{IT}}(t)}$

Insulatard will be modelled using the Berger model. According to this model the amount of remaining insulin in the depot is[8]:

$$A(t) = 100 - \frac{100 \cdot t^s}{T_{50}^s + t^s} \tag{5.2}$$

T_{50} is the time when half of the dose has been absorbed. The linear dependency between the absorbtion halftime and dose size is expressed as:

$$T_{50} = a_{50} \cdot u_{IT}(t) + b_{50} \tag{5.3}$$

Taking the time-derivative of the A gives the rate of absorbtion:

$$\frac{dA}{dt} = \frac{s \cdot t^s \cdot T_{50}^s}{t \cdot (T_{50}^s + t^s)^2} \cdot u_{IT}(t) \tag{5.4}$$

Dividing dA/dt with the distributive volume, V yields the insulin absorbtion rate in $mmol/(liter \cdot time)$.

$$I_{sub_{IT}}(t) = \frac{s \cdot t^s \cdot T_{50}^s}{t \cdot (T_{50}^s + t^s)^2} \cdot u_{IT}(t) \tag{5.5}$$

$$f_{sub}(u_{IT}(t), t) \cdot u_{IT}(t) \tag{5.6}$$

Humalog, $\mathbf{I_{sub_{Hum}}(t)}$

The monomeric insulin is modelled according to the compartment model seen in Fig. 5.3. Taking mass balance for each compartment the following system of equations is given:

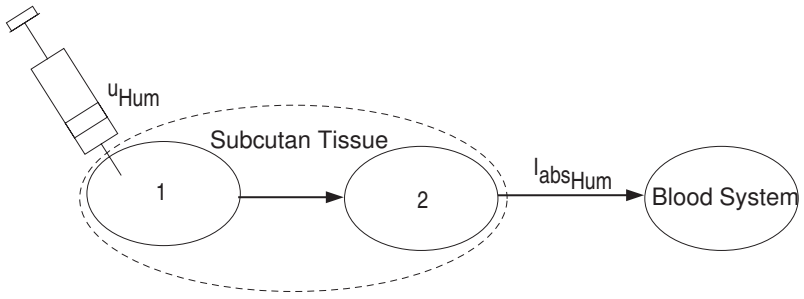

Figure 5.3: Compartment model, Monomeric Insulin.

$$\dot{\mathbf{x}}_{\mathbf{Hum}}(\mathbf{t}) = \begin{pmatrix} -c_1 & 0 \\ c_{12} & -c_2 \end{pmatrix} \cdot \mathbf{x_{Hum}}(\mathbf{t}) + \begin{pmatrix} 1 \\ 0 \end{pmatrix} \cdot \mathbf{u_{Hum}}(\mathbf{t}) \tag{5.7}$$

$$\mathbf{I_{sub_{Hum}}(t)} = \begin{pmatrix} 0 & 1/V \end{pmatrix} \cdot \mathbf{x(t)} \tag{5.8}$$

The transfer function becomes:

$$H_{sub_{Hum}}(s) = C_{Hum} \cdot (s \cdot I - A_{Hum})^{-1} \cdot B_{Hum} \quad (5.9)$$

$$= \frac{c_{12} \cdot 1/V}{(s + c_1) \cdot (s + c_2)} \quad (5.10)$$

Discretization yields:

$$x_{Hum}(k+1) = \begin{pmatrix} d_{11} & 0 \\ d_{21} & d_{22} \end{pmatrix} \cdot x_{Hum}(k) + \begin{pmatrix} b_1 \\ b_2 \end{pmatrix} \cdot u_{Hum}(k) \quad (5.11)$$

$$I_{sub_{Hum}}(k) = \begin{pmatrix} 0 & 1/V \end{pmatrix} \cdot x_{Hum}(k) \quad (5.12)$$

Expressed in discrete transfer function terms:

$$I_{sub_{Hum}}(k) = C_{Hum} \cdot (zI - \Phi_{Hum})^{-1} \cdot \Gamma_{Hum} \quad (5.13)$$

$$= \frac{B_{Hum}(z^{-1})}{A_{Hum}(z^{-1})} \cdot u_{Hum}(k) \quad (5.14)$$

5.1.2 The Glucose Sub-Model

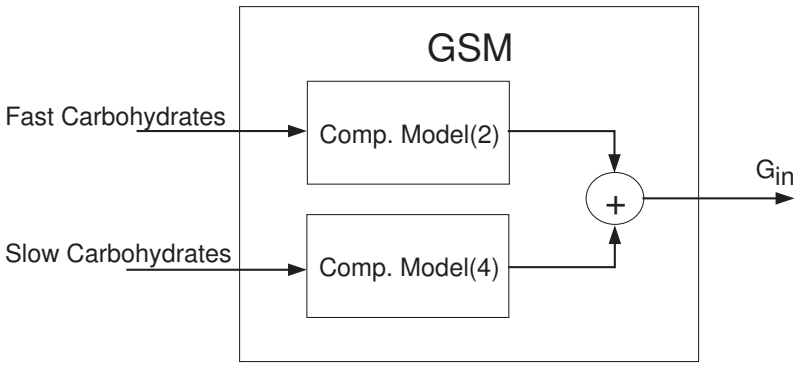

Figure 5.4: The Glucose Sub-Model.

Not much attention has been given to the mathematical modelling of the digestive system. In[22] a complex physiological model is derived where the composition of the meal regarding carbohydrates, proteins and fats are considered. In this thesis, the model will be kept simple, by only looking at the amount of carbohydrates in each meal. The digestive system will be modelled by a compartment model similar to the model developed in [42]. The gastrointestinal tract is considered consisting of a number of compartments. Each compartment interacts with the neighboring compartments. The flow is one-directional, finally reaching the blood compartment. These compartment can be given various physiological interpretations, but such

considerations are not addressed here. Taking mass balance for each compartment the following system of equations is given:

$$\dot{\mathbf{x}}(\mathbf{t}) = \begin{pmatrix} -c_1 & 0 & . & . & . \\ c_{1,2} & -c_2 & 0 & . & . \\ . & . & . & . & . \\ . & 0 & c_{n-2,n-1} & -c_{n-1} & 0 \\ . & . & 0 & c_{n-1,n} & -c_n \end{pmatrix} \cdot \mathbf{x}(\mathbf{t}) + \begin{pmatrix} 1 \\ . \\ . \\ . \\ 0 \end{pmatrix} \cdot u(t) \quad (5.15)$$

$$\mathbf{y} = \begin{pmatrix} 0 & . & . & . & 1/V \end{pmatrix} \cdot \mathbf{x} \quad (5.16)$$

The transfer function for such a system looks like this:

$$H(s) = C \cdot (s \cdot I - A)^{-1} \cdot B \quad (5.17)$$

$$= \frac{c_{1,2} \cdot ... \cdot c_{n-1,n} \cdot 1/V}{(s + c_1) \cdot ... \cdot (s + c_n)} \quad (5.18)$$

The off-diagonal elements are lumped together in the numerator. Thus they can not be separated and will therefore here be set to: $c_0 = c_{1,2} = c_{k-1,k} = c_{n-1,n} = \sqrt[n-1]{c_{1,2} \cdot ... \cdot c_{n-1,n}}$. Values for V are taken from the literature[34].

As previously mentioned the carbohydrate intake has been divided in two parts, fast and slow carbohydrates. The total absorbtion is the sum of these two different absorptions, each modelled as a compartment model with individual order and parameter values.

$$G_{in}(t) = G_{in_{fast}}(t) + G_{in_{slow}}(t) \quad (5.19)$$

How many compartments should be used? According to the initial value theorem[5]:

$$\lim_{t \to 0} G_{in}(t) = \lim_{s \to \infty} s \cdot H_{in}(s) \quad (5.20)$$

The slow carbohydrate must first be digested and splitted into monosaccharides before they can be absorbed. Therefore the absorbtion of slow carbohydrates is very slow in the beginning. At ingestion the flux is thus first at rest implying that G'_{in} is zero as well. At the start of the ingestion the G'_{in} is not changing either, implying that G''_{in} also is zero. Laplace transformation of G''_{in} is $s^2 \cdot H_{in}(s)$. The initial value theorem thus indicates that the relative degree between the numerator and denominator in the $H_{in}(s)$ should be at least of fourth order for this to be fulfilled. Therefore the slow carbohydrates are modelled using a fourth order compartment model. The fast carbohydrates however are modelled with a second order system representing the very fast absorbtion occurring when no splitting has to be undertaken.

Fast carbohydrates, $\mathbf{G_{in_{fast}}(t)}$

Following the discussion above the fast carbohydrates are modelled as:

$$\dot{x}_{fast}(t) = \begin{pmatrix} -c_1 & 0 \\ c_{12} & -c_2 \end{pmatrix} \cdot x_{fast}(t) + \begin{pmatrix} 1 \\ 0 \end{pmatrix} \cdot u_{fast}(t) \quad (5.21)$$

$$G_{in_{fast}}(t) = \begin{pmatrix} 0 & 1/V \end{pmatrix} \cdot x_{fast}(t) \tag{5.22}$$

The transfer function becomes:

$$H_{in_{fast}}(s) = C_{fast} \cdot (s \cdot I - A_{fast})^{-1} \cdot B_{fast} \tag{5.23}$$

$$= \frac{c_{12} \cdot 1/V}{(s + c_1) \cdot (s + c_2)} \tag{5.24}$$

Discretization yields:

$$x_{fast}(k+1) = \begin{pmatrix} d_{11} & 0 \\ d_{21} & d_{22} \end{pmatrix} \cdot x_{fast}(k) + \begin{pmatrix} b_1 \\ b_2 \end{pmatrix} \cdot u_{fast}(k) \tag{5.25}$$

$$G_{in_{fast}}(k) = \begin{pmatrix} 0 & 1/V \end{pmatrix} \cdot x_{fast}(k) \tag{5.26}$$

Written in transfer function mode:

$$G_{in_{fast}}(k) = C_{fast} \cdot (zI - \Phi_{fast})^{-1} \cdot \Gamma_{fast} \tag{5.27}$$

$$= \frac{B_{fast}(z^{-1})}{A_{fast}(z^{-1})} \cdot u_{fast}(k) \tag{5.28}$$

Slow carbohydrates, $\mathbf{G_{in_{slow}}(t)}$

The slow carbohydrates are here modelled with a fourth order compartment model:

$$\dot{x}_{slow}(t) = \begin{pmatrix} -c_1 & 0 & 0 & 0 \\ c_{12} & -c_2 & 0 & 0 \\ 0 & c_{23} & -c_3 & 0 \\ 0 & 0 & c_{34} & -c_4 \end{pmatrix} \cdot x_{slow}(t) + \begin{pmatrix} 1 \\ 0 \\ 0 \\ 0 \end{pmatrix} \cdot u_{slow}(t) \tag{5.29}$$

$$G_{in_{slow}}(t) = \begin{pmatrix} 0 & 0 & 0 & 1/V \end{pmatrix} \cdot x_{slow}(t) \tag{5.30}$$

The transfer function becomes:

$$H_{slow}(s) = C_{slow} \cdot (s \cdot I - A_{slow})^{-1} \cdot B_{slow} \tag{5.31}$$

$$= \frac{c_{12} \cdot c_{23} \cdot c_{34} \cdot 1/V}{(s + c_1) \cdot (s + c_2) \cdot (s + c_3) \cdot (s + c_4)} \tag{5.32}$$

Discretization yields:

$$x_{slow}(k+1) = \begin{pmatrix} d_{11} & 0 & 0 & 0 \\ d_{21} & d_{22} & 0 & 0 \\ d_{31} & d_{32} & d_{33} & 0 \\ d_{41} & d_{42} & d_{43} & d_{44} \end{pmatrix} \cdot x_{slow}(k) + \begin{pmatrix} b_1 \\ b_2 \\ b_3 \\ b_4 \end{pmatrix} \cdot u_{slow}(k) \tag{5.33}$$

$$G_{in_{slow}}(k) = \begin{pmatrix} 0 & 1/V \end{pmatrix} \cdot x_{slow}(k) \tag{5.34}$$

The discrete transfer function becomes:

$$G_{in_{slow}}(k) = C_{slow} \cdot (zI - \Phi_{slow})^{-1} \cdot \Gamma_{slow} \tag{5.35}$$

$$= \frac{B_{slow}(z^{-1})}{A_{slow}(z^{-1})} \cdot u_{slow}(k) \tag{5.36}$$

5.2 Estimating the Sub-Models

Both the glucose and the insulin subsystem dynamics vary significantly between different individuals. Up to 30 percent of interpersonal variation in the insulin absorbtion profiles has been reported[24]. Therefore it is very important to estimate these systems individually. In this section, an attempt is made to find the parameter values for this specific patient using the PEM software in the Identification Toolbox for Matlab.

5.2.1 Initial Estimates

This algorithm needs initial estimates of the parameter values in the submodels. Below some hopefully good suggestions found in the literature are presented.

5.2.2 Insulin Absorbtion

The absorbtion profiles provided by the manufacturers of the insulins, seen in Fig. 2.6 and Fig. 2.7, are not very accurate and should be considered with some scepticism. Instead, profiles provided by the research literature will be looked upon. In Fig. 5.5 two estimates of the absorbtion profile of a monomeric insulin can be seen. Fitting the compartment model to the M4-profile yielded the following dynamical parameters; $c_{11} = c_{22} = 0.3$.

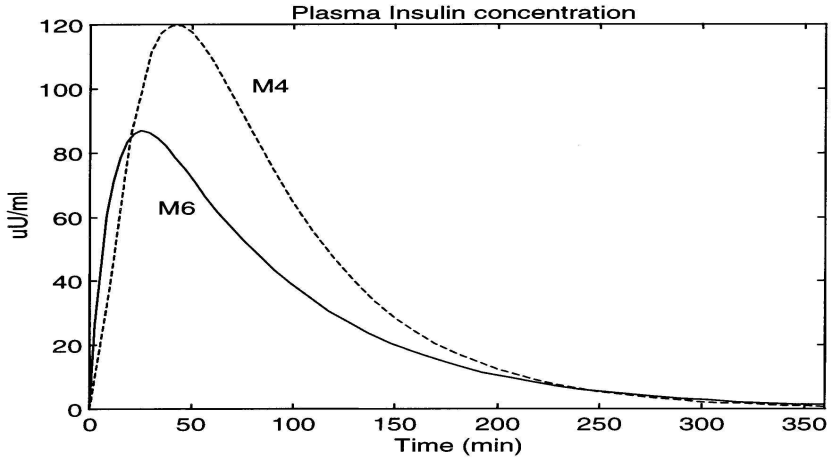

Figure 5.5: Absorbtion profiles of monomeric insulin[36].

The NPH insulin will be modelled using the parameter values found in [36].

5.2.3 Gut Absorbtion

For testing of various models an initial estimate of the gut absorbtion has to be available. Here, absorbtion profiles from the literature will be used as references for the initial estimates.

Fast Carbohydrates

In an oral glucose tolerance test Cobelli has estimated the absorbtion rate from the gut for glucose[34]. Three different models were fitted to the data, and in the picture below the spline model can be seen.

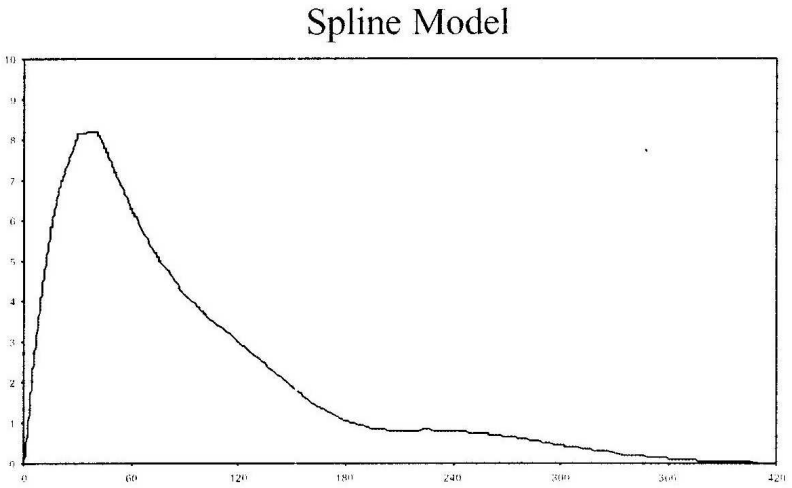

Figure 5.6: Gut Absorbtion, Cobelli's splined data[34].

This corresponds to the fastest carbohydrates here modelled as a second order compartment model. Since no data from the experiment is available no regression can be undertaken, but the following dynamical parameters approximately represents the profile; $c_{11} = 0.3$, $c_{22} = 0.9$.

Slow Carbohydrates

The rate of absorbtion of a mixed meal peaks at 70-90 minutes[26]. A normal meal consists of 10-15 % fast carbohydrates and 85-90 % slow carbohydrates[1]. Bearing this in mind, it seems plausible to argue that the absorbtion peak for slow carbohydrate absorbtion peaks at approximately 1.5 hours. The following set of parameters give a plausible absorbtion profile; $c_{11} = c_{22} = 0.6$ and $c_{33} = c_{44} = 0.5$.

[1] See Appendix A

To find the parameter c_0, which determines the gain of the system, the following relation is considered:

$$V \cdot \int_0^\infty G_{in}\, dt = \eta \cdot C \tag{5.37}$$

Here C is the amount of ingested carbohydrates and η is the efficiency of absorbtion. This relation states that the sum of absorbed carbohydrates equals the sum of ingested carbohydrates minus the loss in the intestine. According to [34] the absorbtion efficiency, η is approximately 86 %.

Given these parameters the absorbtion profiles look like this:

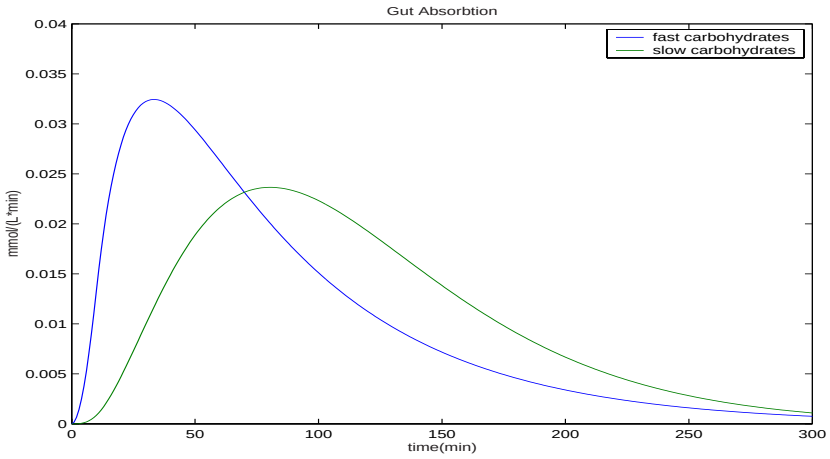

Figure 5.7: Gut Absorbtion, Simulating digestion of 10g fast and 10g slow carbohydrates at t=0.

Another way to get a first estimate of the sub-models is to have a closer look at the correlation between the inputs and the blood glucose change. In Fig. 5.8 the correlation for the slow and fast carbohydrates and the blood glucose change can be seen. Here, the slow carbohydrates seem to act significantly faster than proposed above. The correlation curve for the fast carbohydrates however corresponds quite nicely. This may be explained by the fact that the slow carbohydrates are almost always ingested simultaneously with the fast. The fast carbohydrates, which have a significantly higher gain, thus affect the slow carbohydrates correlation curve making it look faster than it really is.

5.2.4 Glucose/Insulin Interaction Model(GIIM)

To estimate the subsystems a model for the glucose /insulin interaction is needed as well. The simplest model with a physiological interpretation is

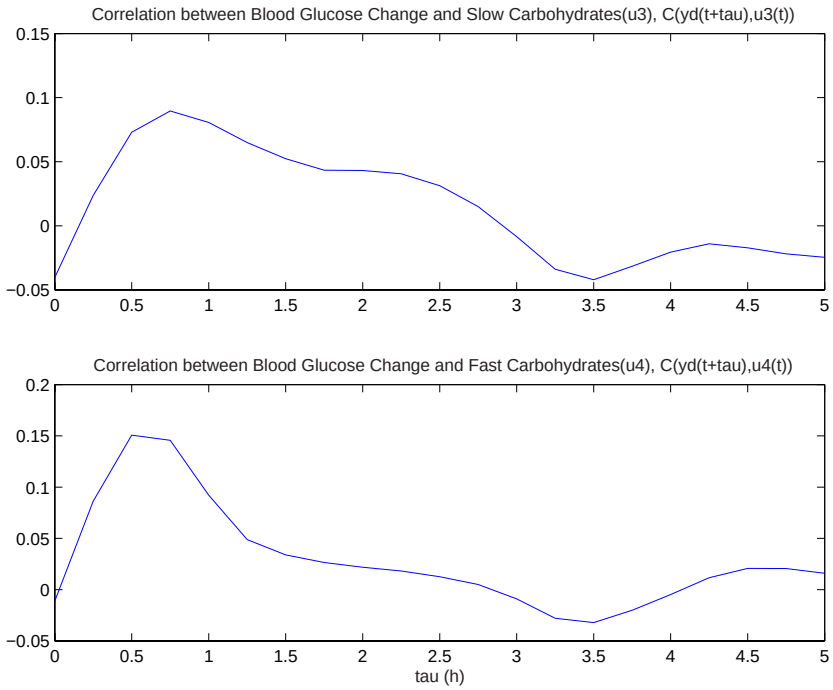

Figure 5.8: Correlation carbohydrate inputs and blood glucose change.

the model proposed by Ackerman[3]:

$$\frac{dG}{dt} = aG(t) + bI(t) + G_{in}(t) \tag{5.38}$$

$$\frac{dI}{dt} = cG(t) + dI(t) + I_{sub}(t) \tag{5.39}$$

where $G(t)$ is the blood glucose concentration and $I(t)$ is the plasma insulin level. Additional states can be added, with or without physiological interpretation, thereby the general linear model is given:

$$\dot{x}_{GIIM} = Ax_{GIIM} + Bu \tag{5.40}$$

$$y = Cx_{GIIM} \tag{5.41}$$

where x_{GIIM} are the different states of the system, and

$$u(t) = \begin{pmatrix} G_{in_{fast}} & G_{in_{slow}} & I_{sub_{Hum}} & I_{sub_{IT}} \end{pmatrix}^T \tag{5.42}$$

and

$$B = \begin{pmatrix} B_1 & B_2 & B_3 & B_4 \end{pmatrix} \tag{5.43}$$

The order of the system was set to 6, based on the discussion in the following chapter, Models and Results.

5.2.5 The Grey-box Total Model

The grey-box estimation method requires that the glucose flux, insulin absorbtion and glucose-insulin interaction is put together into one model. Thus the state space vector is extended:

$$\xi = \begin{pmatrix} x_{Hum} & x_{fast} & x_{slow} & x_{GIIM} \end{pmatrix}^T \tag{5.44}$$

$$\xi(k+1) = \begin{pmatrix} \Phi_{fast} & 0 & 0 & 0 \\ 0 & \Phi_{slow} & 0 & 0 \\ 0 & 0 & \Phi_{Hum} & 0 \\ C_{fast} \cdot B_1 & C_{slow} \cdot B_2 & C_{Hum} \cdot B_3 & A \end{pmatrix} \xi(k) + Bu(k) \tag{5.45}$$

$$y(k) = C \cdot \xi(k) \tag{5.46}$$

where

$$B = \begin{pmatrix} \Gamma_{fast} & 0 & 0 & 0 \\ 0 & \Gamma_{slow} & 0 & 0 \\ 0 & 0 & \Gamma_{Hum} & 0 \\ 0 & 0 & 0 & B_4 \end{pmatrix} \tag{5.47}$$

and

$$u(k) = \begin{pmatrix} u_{fast}(k) & u_{slow}(k) & u_{Hum}(k) & I_{sub_{IT}}(k) \end{pmatrix}^T \tag{5.48}$$

This structure is inserted into the PEM-algorithm. All places in the matrices with initial parameter values are considered as parameters and can be changed by the algorithm. The model is compared with the estimation data and the parameters are changed to find the minimum of the sum of the residuals. Different search algorithm are used to find the global minimum, but of course there is no certainty that the solution is not a local minimum. When looking at the new system, it is apparent that the submodels can not be extracted. However, this is not a major difficulty. The essential parameters affecting the dynamics of the sub-models can still be retrieved. These are the diagonal terms in Φ_{fast}, Φ_{slow} and Φ_{Hum}. The terms in C_{fast}, C_{slow} and C_{Hum} can not be extracted since they are multiplied with the B-matrices of the GIIM. These parameters, together with the non-diagonal terms in the Φ-matrices, determine the gain of the subsystems. Instead these parameters are estimated by considering relation 5.37. This approach may of course result in poor estimates of the gain of the sub-models, but the important relative degree of gain between the parts of the submodels is preserved. The poor estimate of the gains can later be absorbed in the gain of the estimated GIIM. The parameters of the slow acting insulin will not be individually parameterized. The rapid acting insulin is much more important for the dynamics of the system. This, together with the non-linear

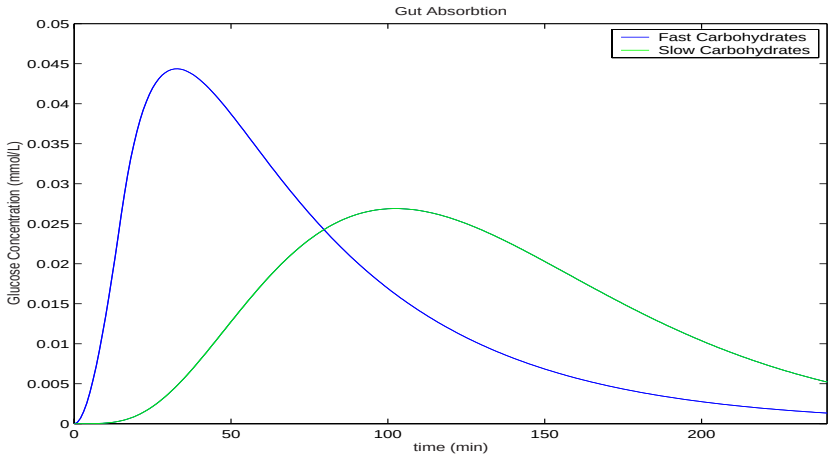

Figure 5.9: Gut Absorbtion.

nature of the slow acting dynamics and the inherent difficulties of identifying such systems, leads to this conclusion. Instead the initial estimate presented above will be used for the characterization of the Insulatard absorbtion.

5.2.6 Results

Estimating the parameters under these conditions gave the set of parameters seen in table 5.1.

Parameters	c_{11}	c_{22}	c_{33}	c_{44}
Humalog	0.2674	0.364	-	-
Fast Carb.	1.175	0.2728	-	-
Slow Carb.	0.5336	0.5164	0.4526	0.4096

Table 5.1: Estimated dynamical parameters.

Simulating the digestion of 10g fast and 10 gram of slow carbohydrates resulted in the absorbtion profiles seen in Fig. 5.9. In Fig. 5.10 The simulation of injecting 10 U Humalog and 10 U Insulatard can be seen. The spectrum of the impulse response from these sub-models can be seen in Fig. 5.11. Incorporating these parameter values in the sub-models the insulin and glucose input can be calculated:

$$I_{sub}(t) = I_{sub_{IT}}(t) + I_{sub_{Hum}}(t) \tag{5.49}$$

$$G_{in}(t) = G_{in_{fast}}(t) + G_{in_{slow}}(t) \tag{5.50}$$

I_{sub} and G_{in} will also be referred to as u_1 and u_2 below. To get an indication of the possibility to use these inputs to explain the behavior in

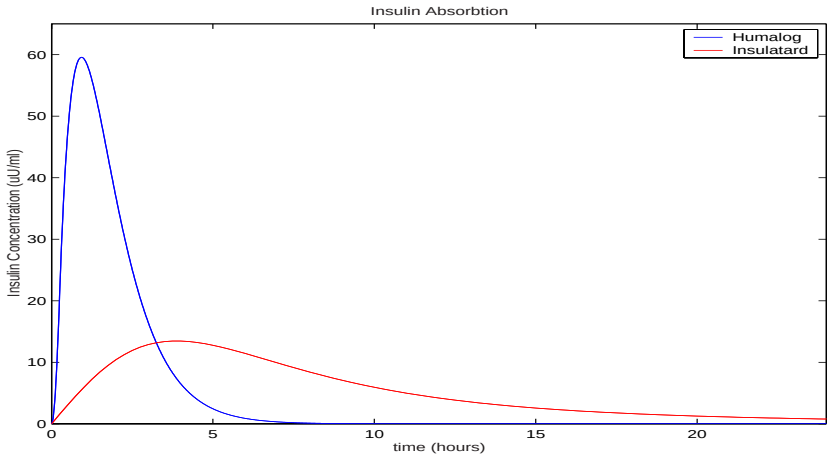

Figure 5.10: Insulin Absorbtion.

the blood glucose the coherence is calculated. In Fig. 5.12 the plain and windowed coherence plots can be seen. The windowed plots indicates that it may be difficult to use these inputs to explain the glucose output. This may be due to a number of factors; high levels of disturbance affecting the system, non-represented inputs and non-linearities in the dynamics.

These parameter values are very close to the initial estimates. This of

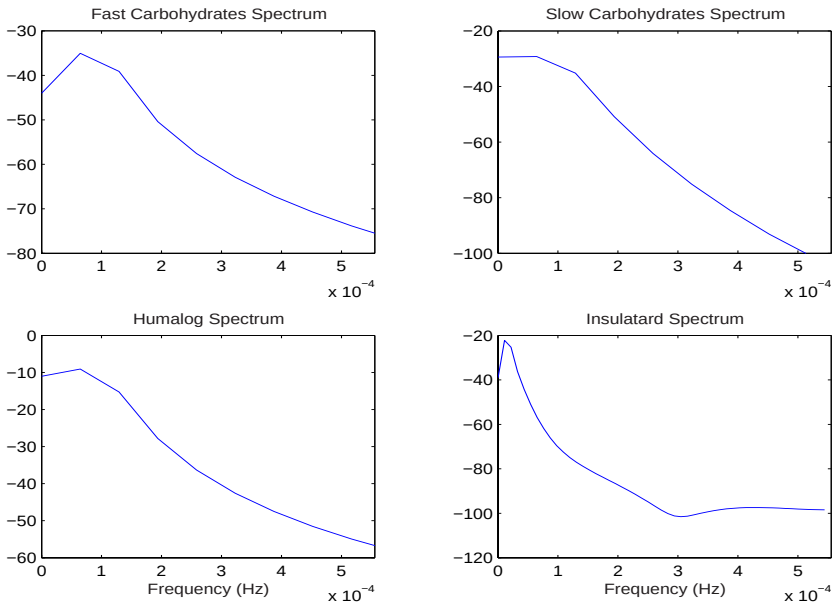

Figure 5.11: Spectrum of submodel parts.

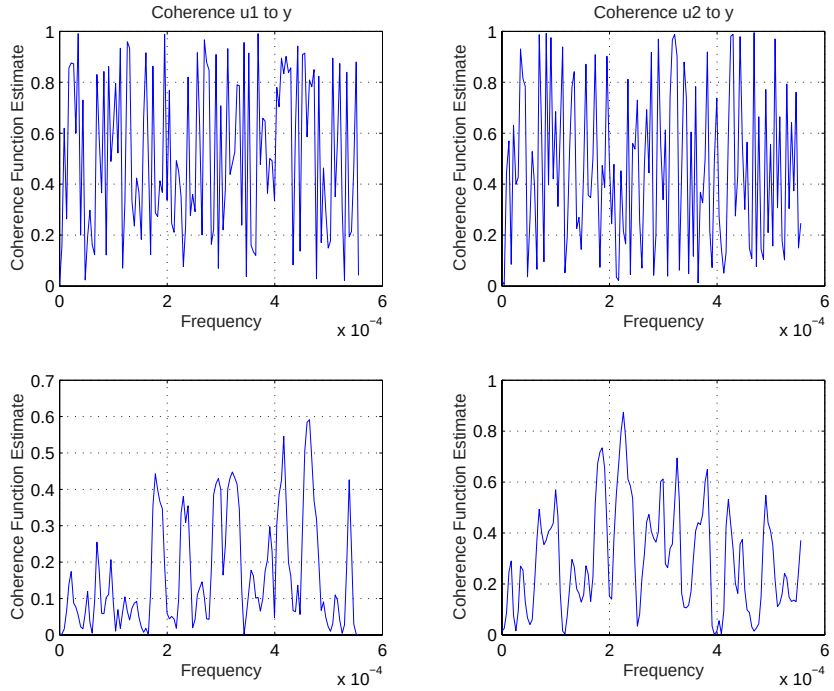

Figure 5.12: In the upper plots the unwindowed coherence plot of the between insulin and glucose inputs and the glucose output and in the lower a Hanning window(L=128) has been used.

course raises the question whether the optimal parameter values have been found. The search for the global minimum might well have ended in a local minimum. Therefore these results should be considered with some scepticism. An other major difficulty already pointed out earlier is that the inputs act simultaneously. This makes it very difficult to extract the influence of each input. This problem is however hard to avoid. Conducting simple experiments where the inputs are separated in time imply unacceptable risks and consequences for the subjects. Good, reliable estimates require clinical experiments such as tracer methods[17] or glucose clamps technics. These are somewhat cumbersome and need medical supervision and are thus not suitable for wider application. Finally the complexity of the models must be considered. Here the glucose subsystem is divided into two models, representing fast and slow carbohydrates. It is a well known fact that the composition of the meal affects the absorbtion. Since this aspect is not represented in the models the ability to describe the absorbtion of different meals may be inadequate.

Chapter 6

Models and Results

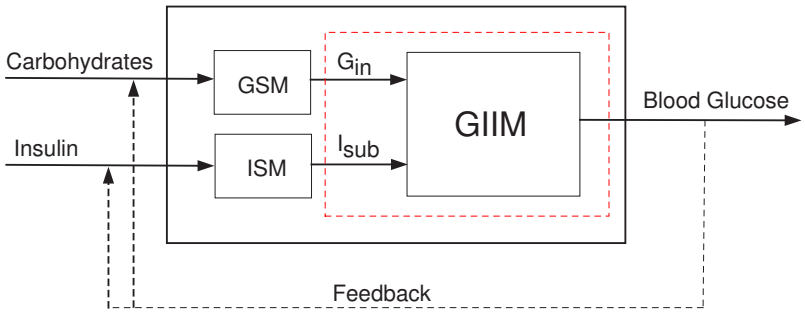

Figure 6.1: The partitioning of the system.

The glucose/insulin dynamic system has been identified to consist of three different main parts; the glucose subsystem, the insulin subsystem and the glucose/insulin interaction. In this chapter the models for the two subsystems and the different black box models used for the glucose/insulin interaction will be presented. After each model the results are reviewed and analyzed. Each model has been estimated using the estimation data and validated with the validation data. The validation has been based on different fitting criteria, such as the Akaike information criteria(AIC) and the final prediction criteria(FPE). The correlation of the residual is also reviewed. Each model has been analyzed with respect to Bode diagrams and pole zero plots to investigate possible pole zero cancellations. The predictive capability of the models is looked upon by comparing the 8-step prediction with the splined data. The Variance Accounted For Criteria(VAF) will serve as a comparative tool. The best model according to this criteria is then subjected to an non-linear transformation, using a simple Wiener model. First, however, the ARMA-model is reviewed. It will serve as a reference for the other models, giving an indication of the benefit of the use of the

sub-models and the different glucose/insulin interaction models.

6.1 ARMA

In the ARMA-model only previous values of the variable of interest is used for the modelling. Attempts to predict future blood glucose values given past and present values have previously been subjected in [12, 6].

$$A(q^{-1}) \cdot y(t) = C(q^{-1}) \cdot e(t) \tag{6.1}$$

This model may help to get an estimate of the approximate degree of the dynamics. First the AR-model is estimated, and thereafter different orders of the C-polynomial are tested.

Here the cost function for the AR-model has been calculated and the Akaike criteria and MDL criteria been evaluated. As can be seen in the Fig. 6.2 all criteria yields the same result; the order of the dynamics is of sixth order.

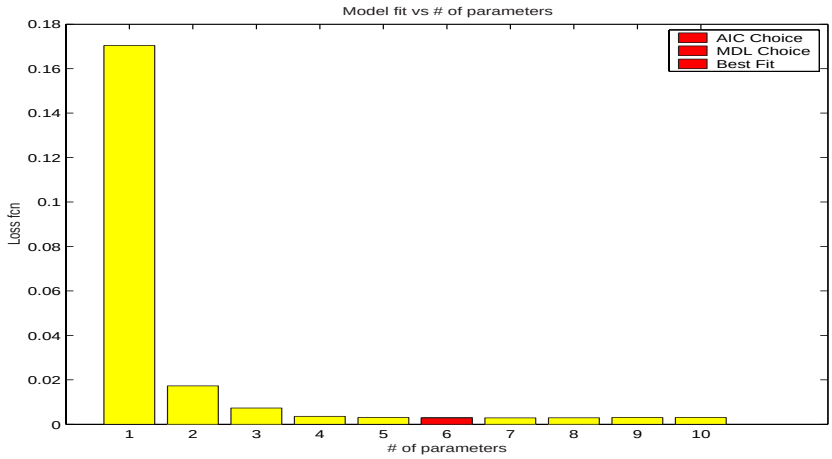

Figure 6.2: Model fit of AR.

Now, to make the prediction error white the C-polynomial is estimated as well. This yields the following model:

$$\begin{aligned} A(q^{-1}) &= 1 - 3.041q^{-1} + 3.71q^{-2} - 2.238q^{-3} && (6.2)\\ &\quad +0.5845q^{-4} + 0.01778q^{-5} - 0.02505q^{-6} && (6.3)\\ C(q^{-1}) &= 1 + 0.453q^{-1} && (6.4) \end{aligned}$$

The correlation function of the residuals can be seen in Fig. 6.3. The correlation function now looks fairly white.

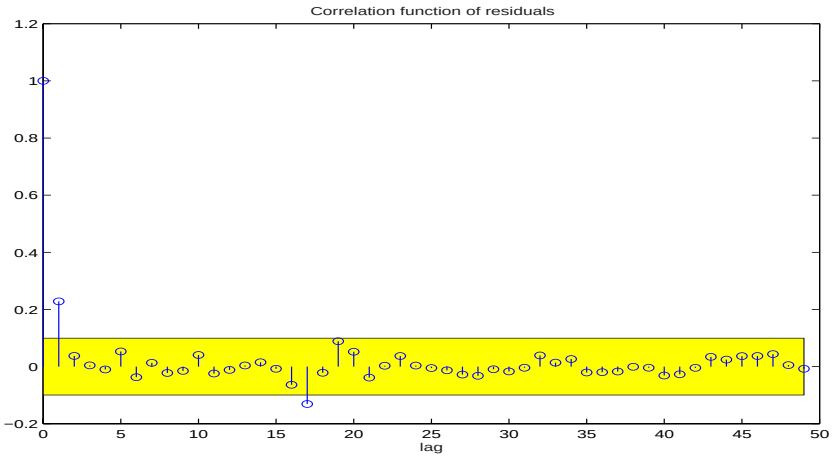

Figure 6.3: Correlation Analysis, ARMA.

In Fig. 6.4, the one step ahead prediction can be seen. The prediction follows the true data almost perfectly. This is however not very surprising considering the high correlation between neighboring glucose values as seen in Fig. 4.8.

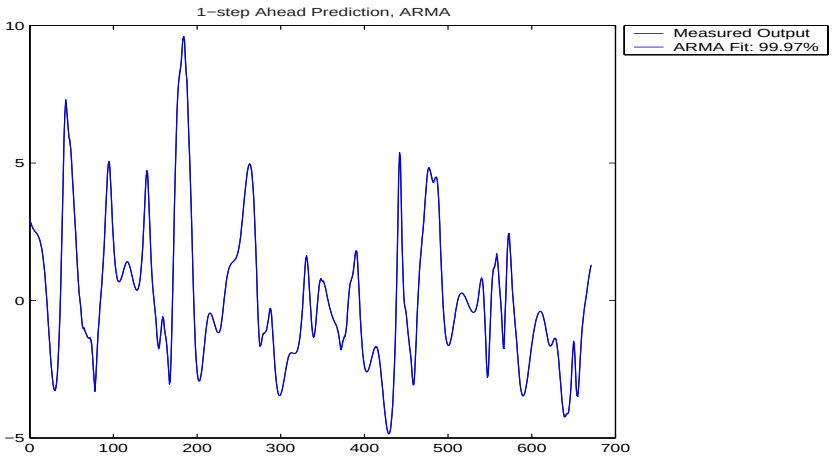

Figure 6.4: 1-step ahead prediction, ARMA.

In Fig. 6.5, a 8-step ahead prediction on the validation data using this model can be seen.

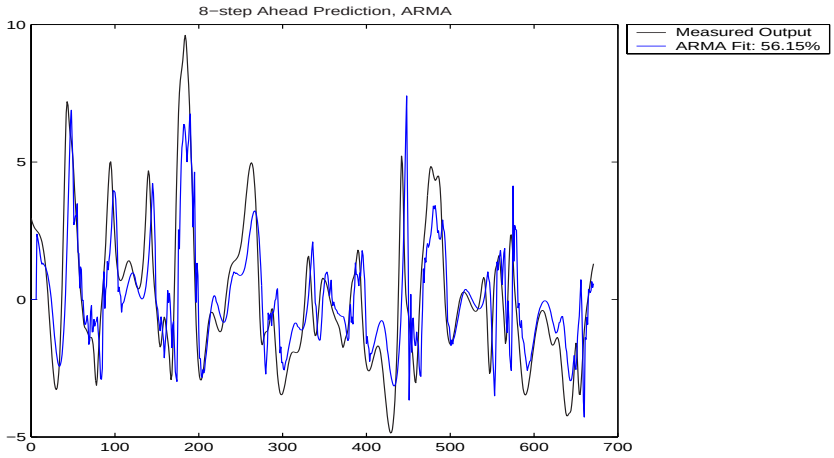

Figure 6.5: 8-step ahead prediction, ARMA.

6.2 Linear Models

6.2.1 ARMAX

ARMAX is a general linear model. Any possible input believed to affect the system can be used. Here, the insulin absorbtion and the glucose flux will be used as inputs.

$$A(q^{-1}) \cdot y(t) = B_1(q^{-1}) \cdot G_{in}(t) + B_2(q^{-1}) \cdot I_{sub}(t) + C(q^{-1}) \cdot e(t) \quad (6.5)$$

Validation

As previously with the AR model different sets of orders of the A- and B-polynomials were tested and evaluated with the validation data. The following sets of system orders and time delays will be tested:

Parameter	Range
n_A	5-10
n_{B_1}	0-3
n_{B_2}	0-3
k_1	0-3
k_2	0-3

The different models are evaluated using the Akaike, MDL and the unmodified cost criteria. In table 6.1 the proposed model structures of the different criteria can be seen.

Noteworthy is that the MDL-criteria indicates that the inputs are not contributing enough to compensate for the added complexity of the model.

Parameter	Loss	MDL	AIC
n_A	6	6	6
n_{B_1}	2	0	1
n_{B_2}	2	0	2
k_1	0	0	2
k_2	3	0	0

Table 6.1: Chosen model structure, ARMAX

Here the model structure selected by the Akaike criteria is chosen. The correlation curve of the residuals can be seen in Fig. 6.6. Apparently the residuals are not white, and thus a noise model has to be estimated. Different orders of the C-polynomial are tested and evaluated according to best fit. This yields the following model:

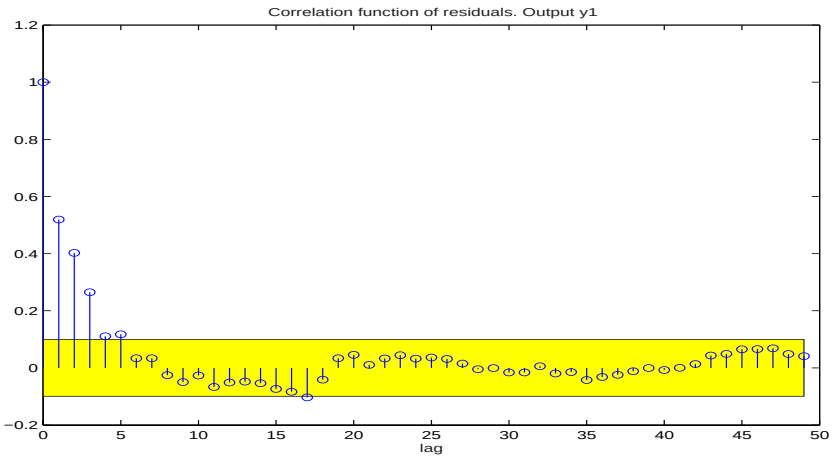

Figure 6.6: Correlation Analysis, ARX.

$$\begin{aligned} A(q^{-1}) &= 1 - 2.817q^{-1} + 3.119q^{-2} - 1.587q^{-3} \\ &\quad +0.1871q^{-4} + 0.1539q^{-5} - 0.04495q^{-6} \\ B_1(q^{-1}) &= -0.2095q^{-2} \\ B_2(q^{-1}) &= 2.917 - 2.569q^{-1} \\ C(q^{-1}) &= 1 + 0.6069q^{-1} \end{aligned}$$

The correlation function of the residuals can now be seen in Fig. 6.7. The residuals are still correlated but the autocorrelation decays more rapidly. The correlation may indicate that the noise dynamics differ from the other system dynamics.

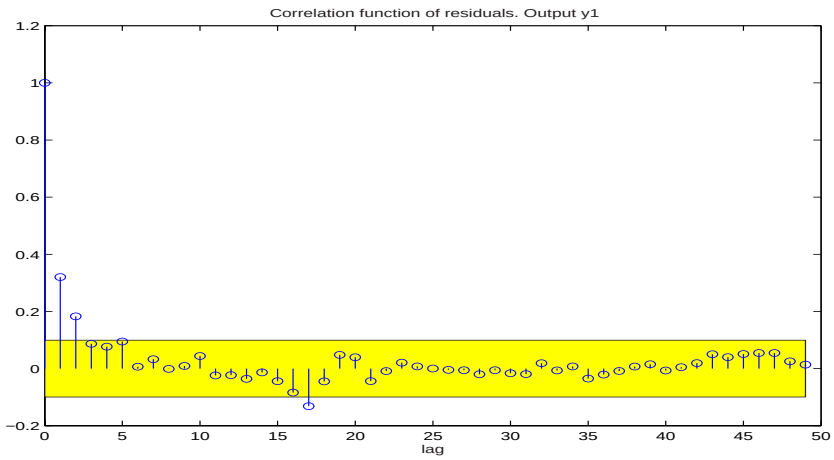

Figure 6.7: Correlation Analysis, ARMAX.

Analysis

In Fig. 6.8 the Bode plot of the system can be seen. Both the Bode plots resemble low pass systems. The cut-off frequency for the insulin input is at approximately 3.2e-5Hz, just above the peak in the Insulatard input spec-

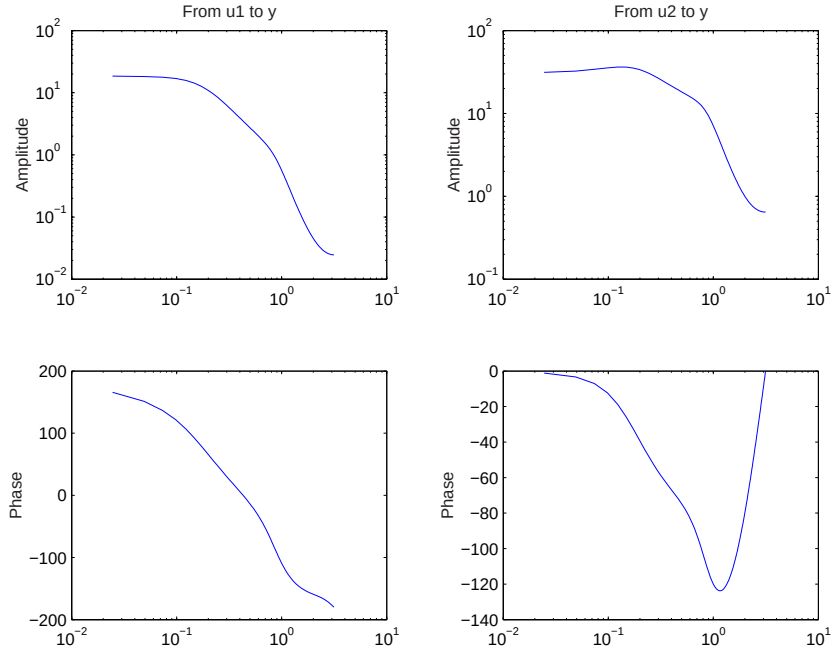

Figure 6.8: Bode Plots, ARMAX.

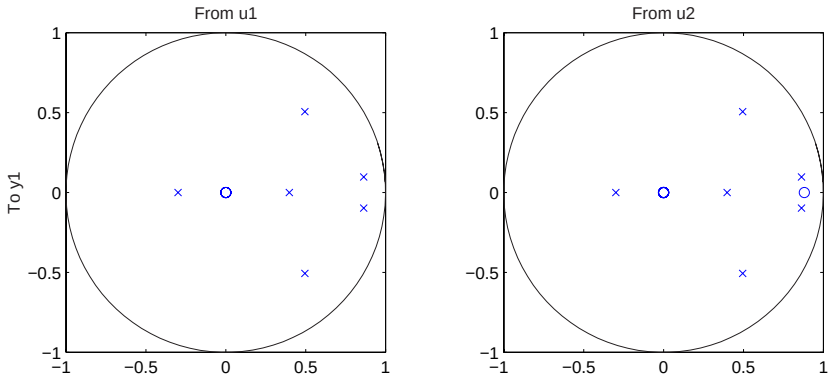

Figure 6.9: Pole/Zero Plot, ARMAX.

trum, which can be seen by looking at Fig. 5.11. However, the magnitude falls relatively slowly implying that the main frequencies of the Humalog input also contribute heavily to the output. The transfer function from glucose input to output also looks somewhat like a low pass system, with a cut-off frequency almost at the spectrum maximum of the fast carbohydrates. The close resemblance between the two transfer functions is due to the low number of zeros. As can be seen from Fig. 6.9 the only difference between the two transfer functions is the zero close to the real one in the glucose/GIIM zero/pole plot.

Prediction

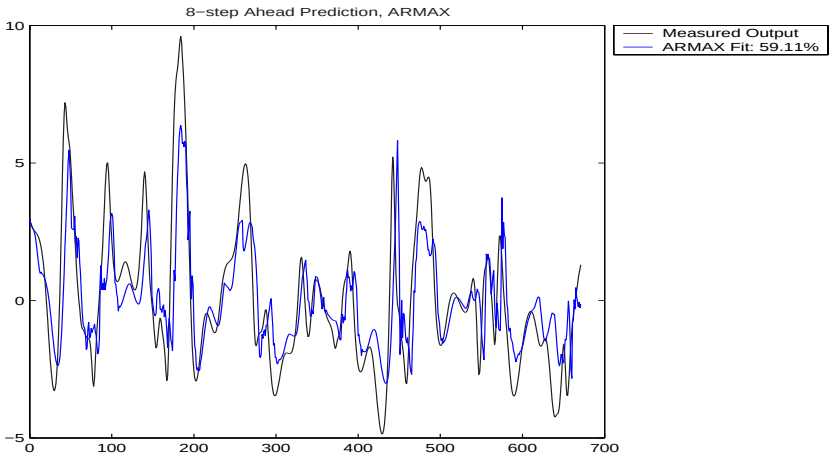

Figure 6.10: 8-step ahead prediction, ARMAX.

In Fig. 6.10 the 8-step ahead prediction using this model can be seen. The improvement from the ARMA-model is quite small.

6.2.2 Weighted Least Squares

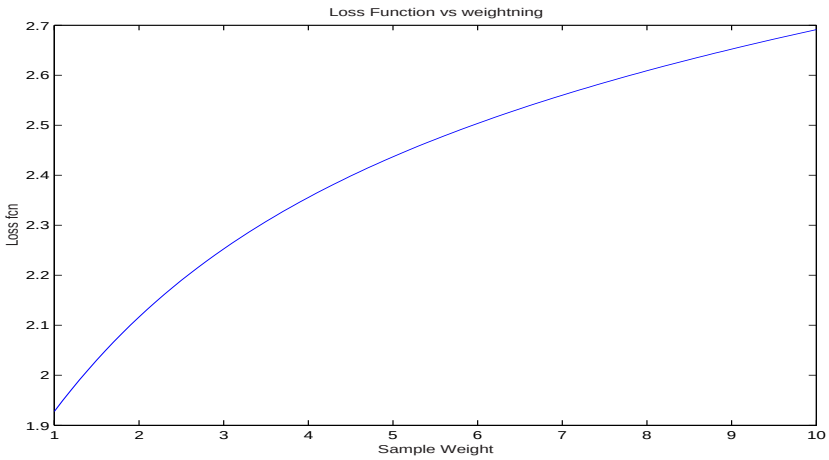

Figure 6.11: Loss function versus Weight.

The data used is very scarce. Most of the blood glucose values used during the estimation and validation are interpolated from a few measurements. By interpolation there is a risk of introducing false dynamics resulting in invalid parameter estimates. Therefore, it may be an idea to valuate the measured blood glucose values higher than the interpolated values during the estimation process. This is done by introducing a weighting matrix into the parameter calculations. Different weighting values are tested to investigate whether the model improves when the real measurements are given a higher weight. The evaluation criteria used is the loss function. In Fig. 6.11 the loss function versus the ratio between the weight of the sampled data and the weight of the interpolations can be seen. The loss function increases as the ration increases. Thus, no improvement can be seen by weighting the real measurements heavier than the interpolated values.

6.2.3 Subspace Model

Validation

To find the best model different model orders and different orders of s were tested and evaluated using the cost function, the AIC and the FPE Criteria. The result can be seen in table 6.2.

Table 6.2: Comparison SMI-models; best, second best, third best

n	4			5			6			7		
s	Loss	AIC	FPE	Loss	AIC	FPE	Loss	AIC	FPE	Loss	AIC	FPE
6	4.025	1.405	4.074	0	0	0	0	0	0	0	0	0
7	5.506	1.718	5.572	6.705	1.918	6.805	0	0	0	0	0	0
8	7.331	2.004	7.419	8.038	2.099	8.159	2.754	1.031	2.804	0	0	0
9	10.33	2.347	10.45	9.095	2.223	9.231	4.259	1.467	4.336	17.59	2.888	17.96
10	13.58	2.62	13.74	13.16	2.592	13.36	6.39	1.873	6.505	26.85	3.311	27.42
11	16.35	2.806	16.55	15.81	2.776	16.05	8.965	2.211	9.126	11.06	2.424	11.29
12	22.51	3.126	22.78	17.36	2.869	17.62	14.07	2.662	14.32	19.82	3.007	20.23
13	0	0	0	18.74	2.946	19.02	20.01	3.014	20.37	31.29	3.464	31.95
14	0	0	0	21.26	3.072	21.58	22.38	3.126	22.79	31.54	3.472	32.21
15	0	0	0	23.79	3.184	24.15	18.31	2.925	18.64	29.22	3.396	29.83
16	0	0	0	0	0	0	14.23	2.673	14.49	25.13	3.245	25.66
17	0	0	0	0	0	0	15.42	2.754	15.7	23.55	3.18	24.05
18	0	0	0	0	0	0	24.39	3.212	24.83	21.07	3.069	21.52
19	0	0	0	0	0	0	0	0	0	22.22	3.122	22.69
20	0	0	0	0	0	0	0	0	0	23.22	3.166	23.7
21	0	0	0	0	0	0	0	0	0	24.35	3.213	24.86

Table 6.3: Comparison SMI-models, cont.

n	8			9			10		
s	Loss	AIC	FPE	Loss	AIC	FPE	Loss	AIC	FPE
10	25.134	3.248	25.74	0	0	0	0	0	0
11	23.196	3.1678	23.755	95.252	4.5833	97.838	0	0	0
12	18.559	2.9448	19.007	70.457	4.2818	72.37	199.19	5.324	205.21
13	23.192	3.1676	23.751	51.55	3.9693	52.949	137.39	4.9526	141.54
14	19.519	2.9952	19.989	77.897	4.3822	80.011	68.625	4.2584	70.698
15	18.725	2.9536	19.176	61.098	4.1393	62.757	51.555	3.9724	53.113
16	17.75	2.9002	18.178	32.624	3.5118	33.51	25.703	3.2764	26.48
17	18.122	2.9209	18.559	36.917	3.6355	37.919	25.185	3.256	25.946
18	19.92	3.0155	20.4	50.396	3.9467	51.764	32.141	3.4999	33.112
19	18.94	2.9651	19.397	38.752	3.684	39.804	19.591	3.0048	20.182
20	16.973	2.8554	17.382	31.636	3.4811	32.494	20.97	3.0729	21.604
21	16.913	2.8519	17.321	27.568	3.3434	28.317	21.064	3.0773	21.701
22	21.079	3.0721	21.587	22.546	3.1423	23.158	22.302	3.1344	22.975
23	25.108	3.247	25.713	17.82	2.9071	18.304	22.032	3.1222	22.697
24	27.213	3.3275	27.869	15.713	2.7813	16.14	20.834	3.0664	21.464
25	0	0	0	16.474	2.8286	16.921	19.923	3.0217	20.525
26	0	0	0	18.502	2.9446	19.004	22.195	3.1296	22.865
27	0	0	0	21.435	3.0918	22.017	23.925	3.2047	24.648
28	0	0	0	0	0	0	21.143	3.0811	21.782
29	0	0	0	0	0	0	21.479	3.0969	22.128
30	0	0	0	0	0	0	24.579	3.2317	25.322

Analysis

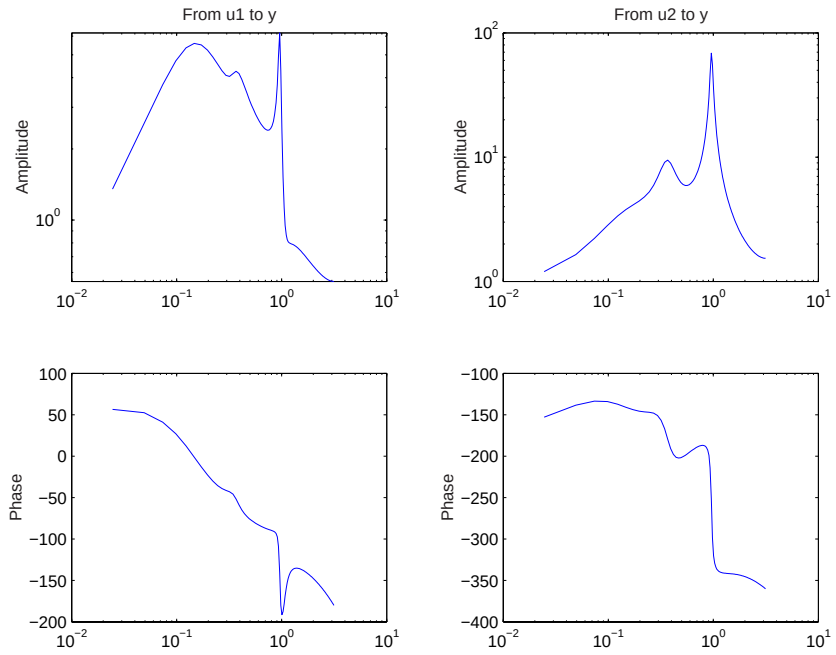

Figure 6.12: Bode Plots, Subspace Model(n=6, s=9).

The best model according to the criteria is n=6 with s=8. However, this model is unstable with a pole-pair outside the unit circle. The third best model is also of sixth order, but stable. The Bode plot can be seen in Fig. 6.12. Looking at the insulin/GIIM Bode diagram three peaks can be identified. The first peak is the product of the pole pair close to the real one.

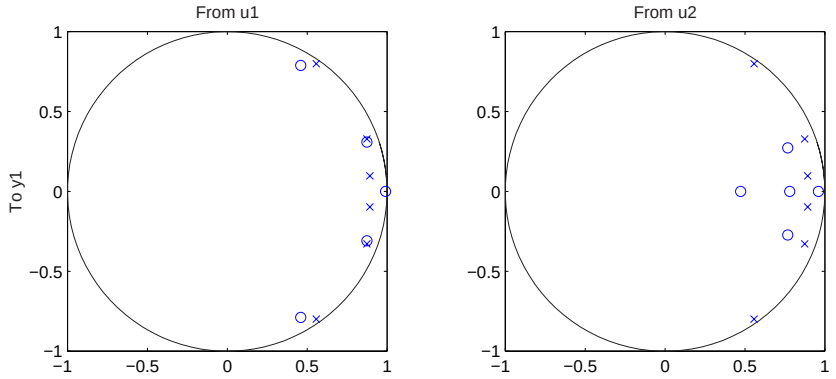

Figure 6.13: Pole/Zero Plot, Subspace Model(n=6, s=9).

The second small peak and the following fall in amplitude is due to the near pole/zero cancellation seen in the right plot of Fig. 6.13. The last sharp peak at 10^0 followed by the drastic fall in amplitude can be explained by the pole/zero pair lying very close to each other at $0.5 \pm 0.8i$. In the second Bode plot the resonance peak at the low frequency has been eliminated by the zero at 0.8. Instead, the middle frequency peak is more distinct followed by the drop in amplitude. In this case the poles and zeros are not cancelling each other but lie quite close to each other. The poles at $0.5 \pm 0.8i$ are now left alone resulting in a distinct resonance peak at 10^0.

The second best model, n=4, s=6, is also the smallest model. Here the pole/zero pairs that caused the peaks at 10^0 in the transfer functions are excluded as can be seen in Fig. 6.14 and Fig. 6.15. Only the most essential dynamics are left. The insulin transfer function is now totally dominated by the pole pair close to the real one. The small peak at 0.6-0.7 is due to the near cancellation of the poles at $0.7 \pm 0.6i$. The glucose transfer function on the other hand has a distinct peak at 0.6-0.7 rad/15min, caused by the this pole pair. This peak is somewhat of a average between the two peaks seen in the higher order model.

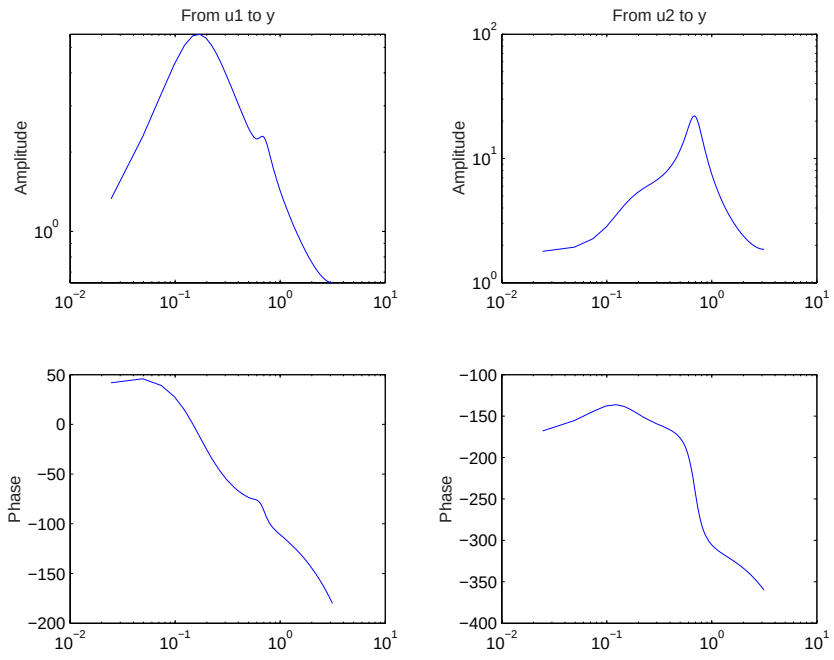

Figure 6.14: Bode Plots, Subspace Model(n=4, s=6).

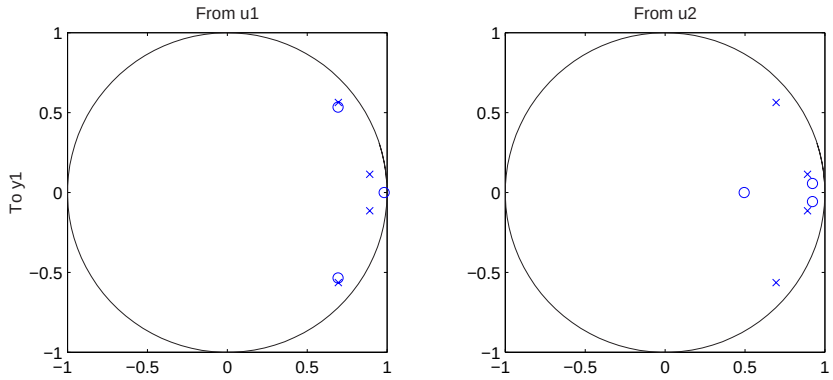

Figure 6.15: Pole/Zero Plot, Subspace Model(n=4, s=6).

Prediction

The predictive capability of the subspace models are not very impressive. In Fig. 6.16, the 8-step prediction of the n=6,s=9 can be seen. The VAF is significantly lower than for the ARMAX-model.

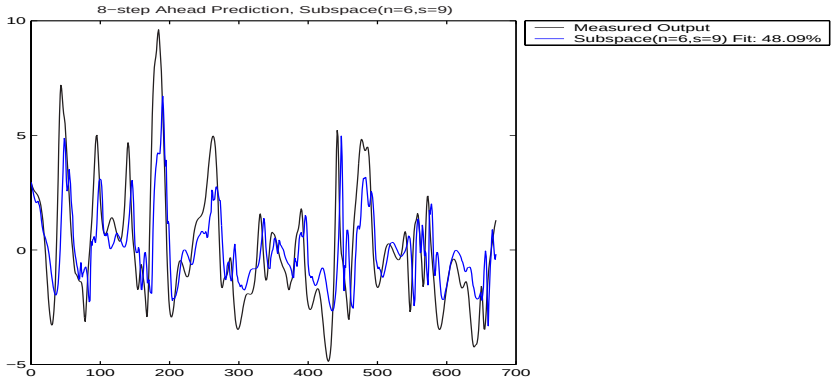

Figure 6.16: 8-step ahead prediction, Subspace.

6.2.4 The General Transfer Function Model(GTFM)

Considering the suspected pole/zero cancellations and the high level of correlation in the residuals in the previous models it may be an idea to consider separating the dynamics in the system. By the general transfer function model the different inputs and the noise model all have different dynamics:

$$A(q^{-1}) \cdot y(t) = \frac{B_1(q^{-1})}{F_1(q^{-1})} \cdot u_1 + \frac{B_2(q^{-1})}{F_2(q^{-1})} \cdot u_2 + \frac{C(q^{-1})}{D(q^{-1})} \cdot e(t) \qquad (6.6)$$

Validation

The model was estimated for the sets of orders in table 6.4. The validation

n_A	n_{B_1}	n_{B_2}	n_{F_1}	n_{F_2}	n_C	n_D	k_1	k_2
3-6	2-3	2-3	2-3	2-3	0-3	0-3	0-2	0-2

Table 6.4: Sets of system orders to evaluate

criteria all selected the model structure seen in table 6.5.

n_A	n_{B_1}	n_{B_2}	n_{F_1}	n_{F_2}	n_C	n_D	k_1	k_2
5	2	3	1	1	3	2	0	0

Table 6.5: Chosen model structure, GTFM.

Estimating the parameters gave this model:

$$
\begin{aligned}
A(q^{-1}) &= 1 - 3.209q^{-1} + 4.257q^{-2} - 2.966q^{-3} + 1.087q^{-4} - 0.1613q^{-5} \\
B_1(q^{-1}) &= -0.03211 + 0.01213q^{-1} \\
B_2(q^{-1}) &= 0.9626 - 1.414q^{-1} + 0.5386q^{-2} \\
F_1(q^{-1}) &= 1 - 0.01277q^{-1} + 0.5702q^{-2} - 0.6425q^{-3} \\
F_2(q^{-1}) &= 1 + 0.4967q^{-1} - 0.06102q^{-2} \\
C(q^{-1}) &= 1 + 0.4572q^{-1} \\
D(q^{-1}) &= 1 + 0.1633q^{-1}
\end{aligned}
$$

The residuals are now almost uncorrelated as can be seen in Fig. 6.17.

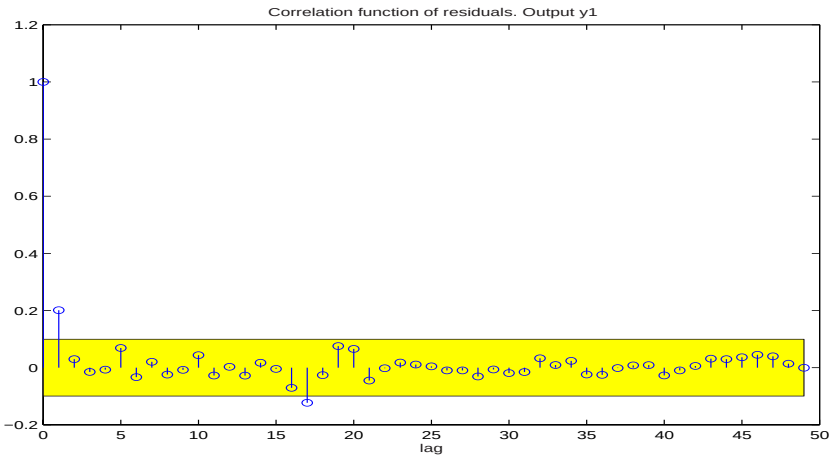

Figure 6.17: Correlation Analysis, General Transfer Function Model.

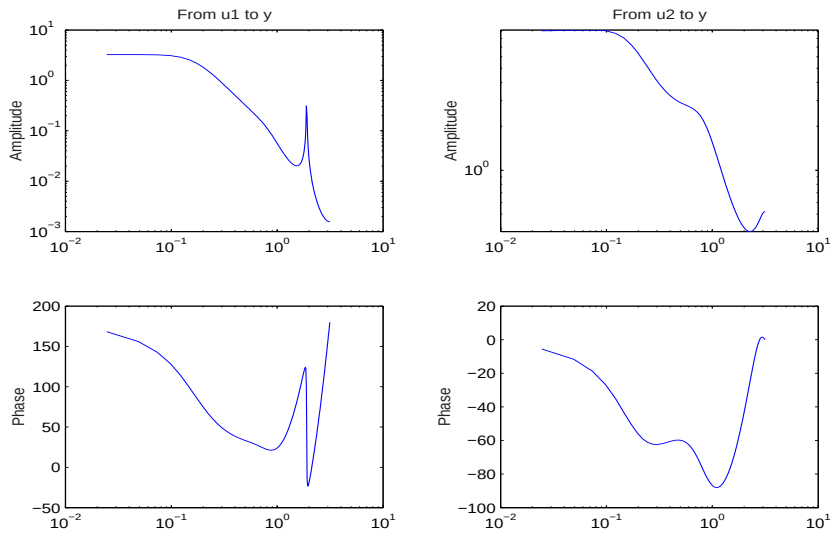

Figure 6.18: Bode diagrams, GTFM.

Analysis

In Fig. 6.18 the Bode diagrams can be seen. The first Bode plot looks like a low pass system except for the interruption of the sharp resonance peak at a high frequency. This resonance is due to the odd, almost undamped pole pair at $-0.3 \pm 0.9i$, see Fig. 6.19. The second Bode plot also resembles a low pass system. From the pole/zero map the different poles associates with each input can be seen quite clearly. The poles not relevant for the input are nicely cancelled.

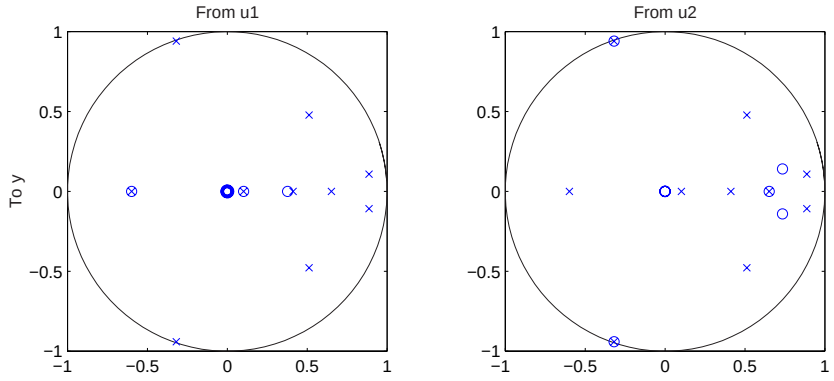

Figure 6.19: Zero/Pole Plot, GTFM.

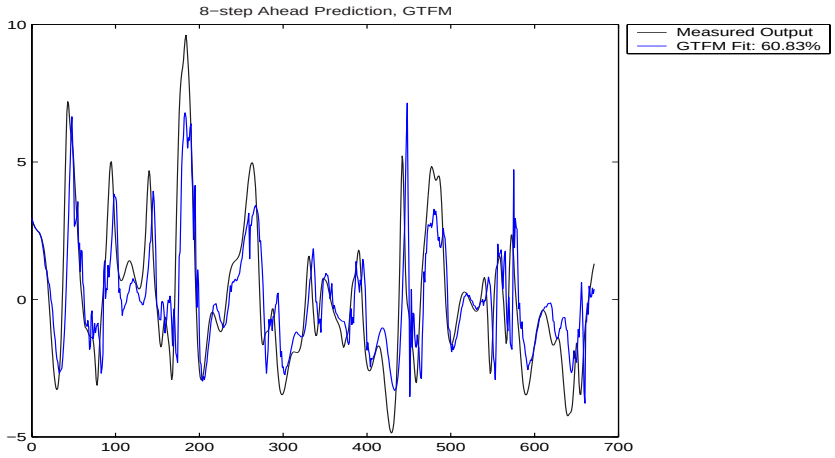

Figure 6.20: 8-step ahead prediction, General Transfer Function Model.

Prediction

The predictive capability, Fig. 6.20 is improved somewhat compared to the ARMAX-model.

6.2.5 Comparison

In this section the previous models will be compared, looking at Bode plots, zero/pole plots and predictive capability.

Analysis

In Fig. 6.21 and Fig. 6.22 a comparison between the Bode plots of the previous models can be seen. The transfer functions fall into two separate categories; the subspace models and the ARMAX and GTFM models. The subspace models put more emphasis at the higher frequencies, while the ARMAX and GTFM have a typical low pass performance. Since these models have the best predictive capability, they probably also best resemble the true system. Therefore focus will be on these two models. There are some important differences between the models. There is a resonance peak in the insulin/GIIM transfer function in the GTFM not present in the ARMAX model. An other difference is the noise dynamics. In the ARMAX model the residuals are still correlated, while in the GTFM they are practically uncorrelated. This may in part be explained by the GTFM:s general better ability to explain the system using the inputs, but also by having a slightly different noise model as can be seen in Fig. 6.24 and Fig. 6.25.

In all the models of the insulin/GIIM dynamics the pole pair close to the real one is present. Likewise all models agree that the glucose/GIIM transfer

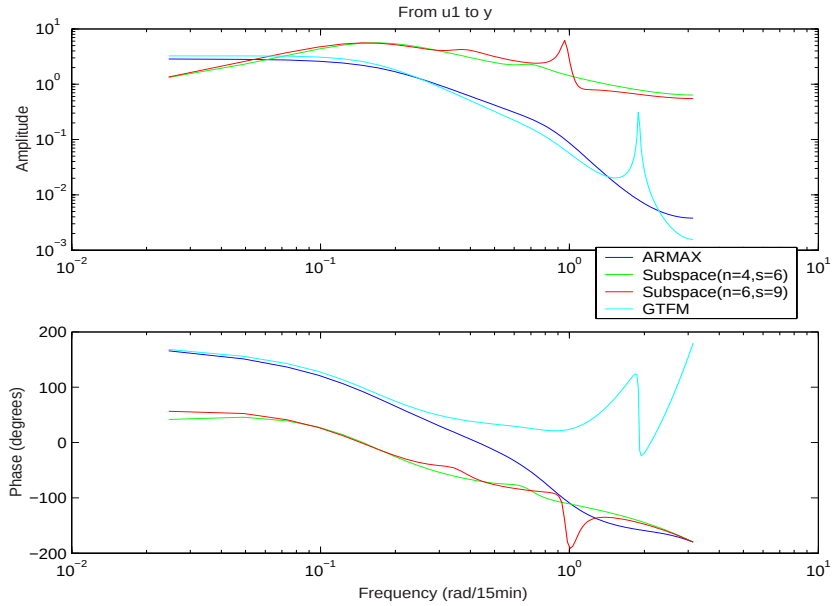

Figure 6.21: Comparison Bode plot, ISM/GIIM.

function has a pole pair somewhere in the vicinity of $0.5 - 0.6 \pm 0.5 - 0.8i$.

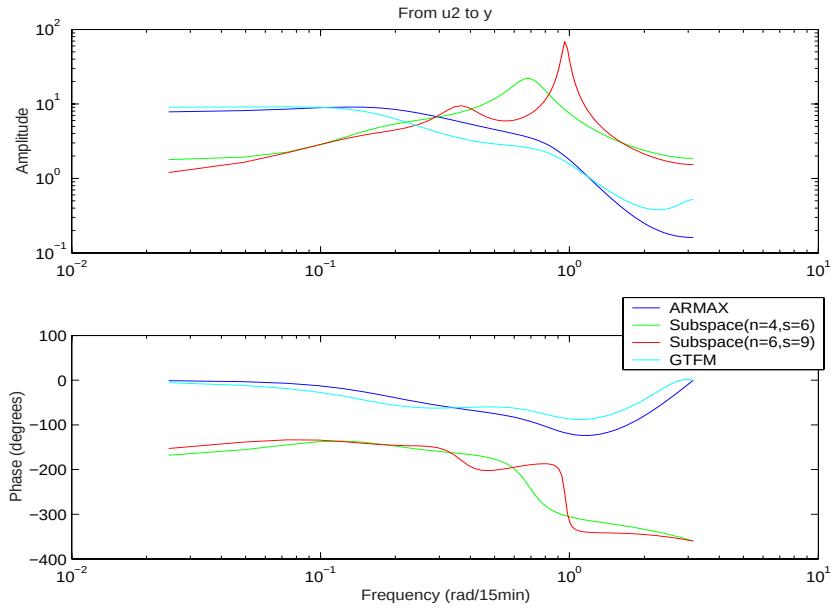

Figure 6.22: Comparison Bode plot, GSM/GIIM.

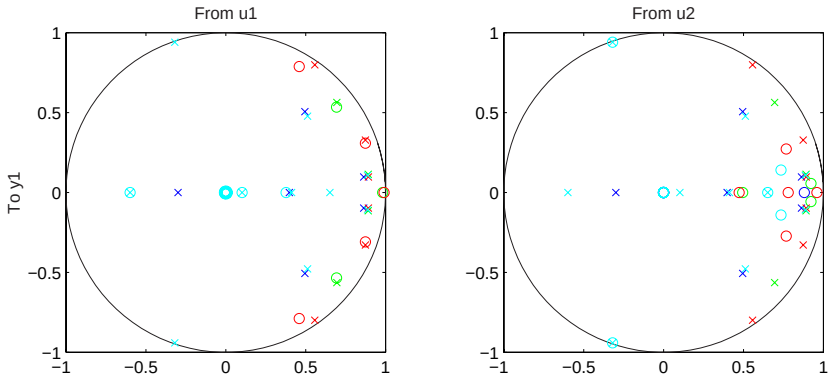

Figure 6.23: Comparison zeros and poles, ARMAX, Subspace(n=4,s=6), Subspace(n=6,s=9) and GTFM

This may indicate that these dynamics are essential parts of the system.

Prediction

The best model according to VAF for the 8-step prediction is the GTFM. In Fig. 6.26 the models' prediction error standard deviation can be seen for predictions between 1 and 10 steps forward. Apparently, the GTFM is the best model in the whole range. The result is however not very impressive; the best linear model is obviously not capable of describing the system very well. By looking closely at the prediction and and comparing it with the real signal a lag can be seen. This lagging of the prediction can also be seen

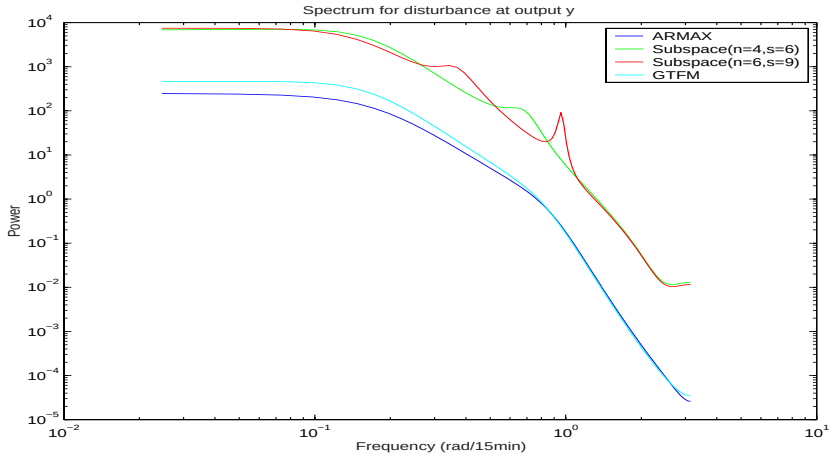

Figure 6.24: Bode plot, Noise Dynamics.

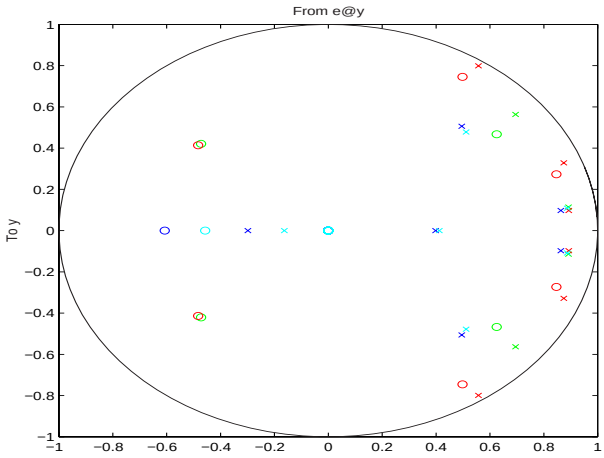

Figure 6.25: Zeros and poles of the noise models, ARMAX, Subspace(n=4,s=6), Subspace(n=6,s=9) and GTFM.

by studying the correlation between the prediction and the real signal. In Fig. 6.27 the correlation can be seen. Looking at the correlation it can be determined that the lag is about 75 min.

The predictive capacity degrades very fast as seen in Fig. 6.26. This can be seen even clearer by looking at the plots in Fig. 6.28. After already 4 steps the model has difficulties with under- and overshoots. After 8 steps these problems have escalated making the predictions very poor. In the last plot the pure simulation can be seen. In Fig. 6.29 the simulation can be seen clearer. In the upper plot the simulated data and the splined data can

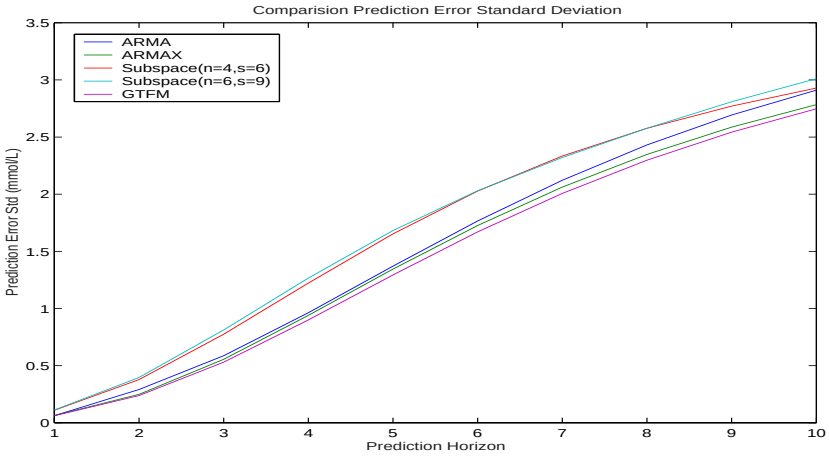

Figure 6.26: The prediction standard deviation vs prediction horizon.

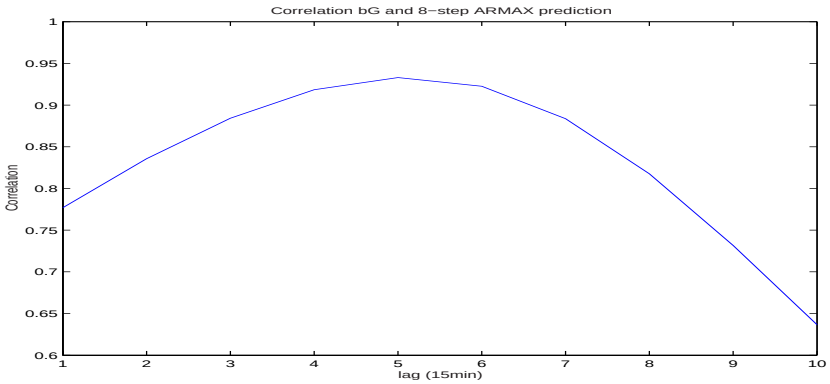

Figure 6.27: The prediction lags the real data

be seen again. The model has obvious problems with the magnitude. In the lower plot the output of the model has simply been scaled with a factor of 2.5. Now it is easier to see where the model reacts totally wrong and where it is more on track. At many instances the model reacts qualitatively right but with too small magnitude. At other times the model deviates seriously qualitatively wrong. The reasons for this are several:

- The system is highly **non-linear** in its responses to inputs. Already for the 8-step prediction the model has severe difficulties coping with the high peaks and the deep bottoms.

- there may be and probably are **unrepresented inputs** having a serious impact on the output. Such inputs may be exercise and alcohol intake.

- The **data** used may be incomplete and flawed. The data was collected during 6 months in a diabetes diary. The size and timing of each meal sometimes had to be noted afterwards. Many meals, especially snacks are thus not represented correctly.

- The **interpretation** of the data is quite arbitrary. The predefined meals[1] are very coarse estimates and do not span the range of intake sufficiently.

- **The interpolation** of the glucose measurements. The interpolation routine used may be a poor method to reconstruct the data and thus introduce false dynamics in the time series.

[1]See Appendix A

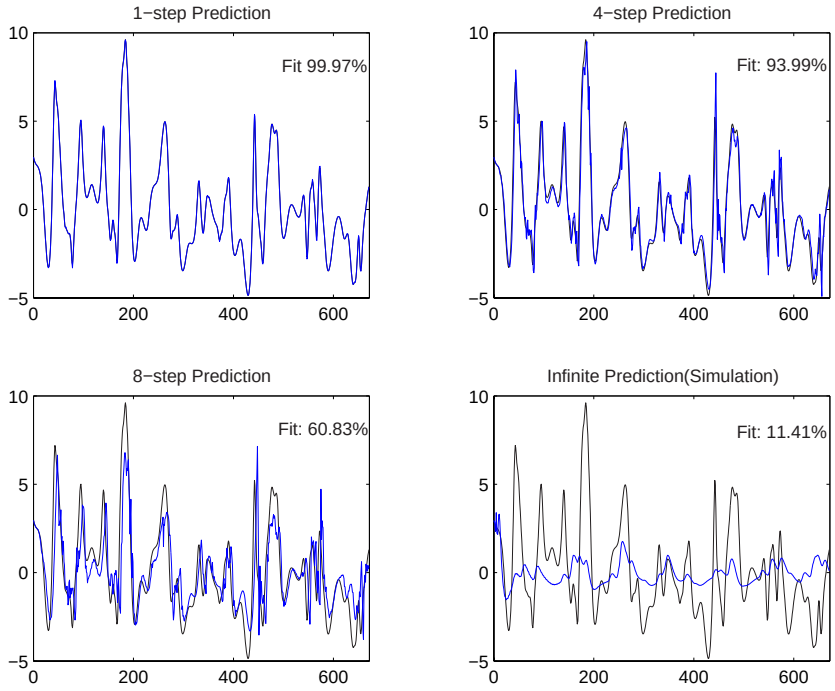

Figure 6.28: Illustration of the degradation of predictive capacity, GTFM.

- The system may have **time dependant dynamics**. That this is the case in a longer time frame was seen in the Data chapter, but there is also evidence that the dynamics differ over the time of the day.

- **The sub-models** are very simplistic and may be inappropriate to fully characterize the glucose and insulin flux. Especially the GSM is far to simplified to accurately describe the digestion and absorbtion of food.

- The is a considerable **intrapersonal variability** in the absorbtion of insulin. This is probably true to some extent for the glucose absorbtion as well. This constitutes an uncertainty that can not be modelled.

These factors not only cause anomalies in the pure simulation case, but also severely hampers the estimation and validation processes.

Finally let's take a look at the simulated data once more. In Fig. 6.30 the simulated data has been simulated by using varied inputs; $u_{i,sim} = (1 \pm 0.25)u_i$. This is supposed to represent the natural uncertainty in the absorbtion processes.

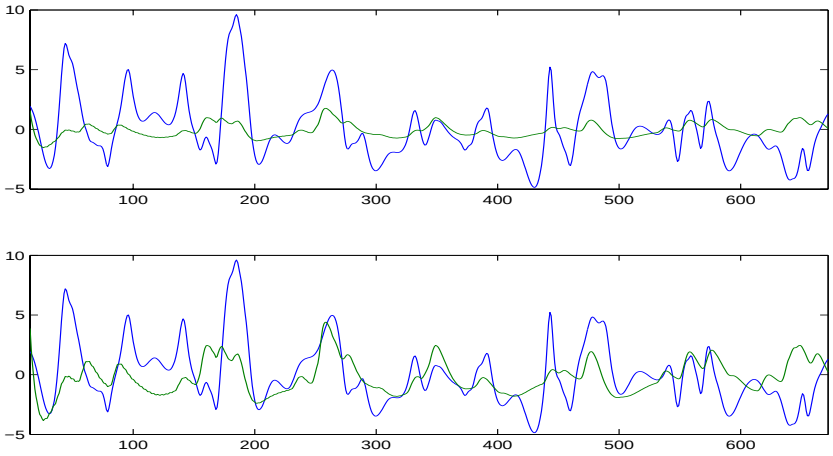

Figure 6.29: The upper plot: Simulated Data(GTFM) and real data; Lower plot: Scaled Simulated Data and real data.

6.3 Non-linear Models

Since the linear models proved insufficient to represent the system non-linear models must be considered. Here a number of possible opportunities for making the models non-linear are considered. First of all the data can be transformed before the linear models are applied. Two different transformations of the blood glucose data are looked upon below. An other possibility is the Hammerstein and Wiener models. A Hammerstein model is basically a non-linear transformation of the inputs thereafter the normal linear models are used. Some simple transformations are considered in the NARMAX section below. The Wiener model consists of making a non-linear transformation of the output of the linear model. In the GTFM-Wiener model section below Chebychev polynomials are considered for such a non-linear function of the output.

6.3.1 Data Transformations

In the data chapter the log-normal character of the blood glucose samples was investigated. A test of log-normality was undertaken, and passed for p¡0.01. Thus a natural non-linear transformation is to take the natural logarithm of the glucose data.

$$y_{log} = \log(y) \tag{6.7}$$

This concept has been tested for all the models discussed above, but without improvement. An other transformation proposed by Kovatchev in [30] is:

$$y_{kov} = 1.794(\log(y)^{1.026} - 1.861) \tag{6.8}$$

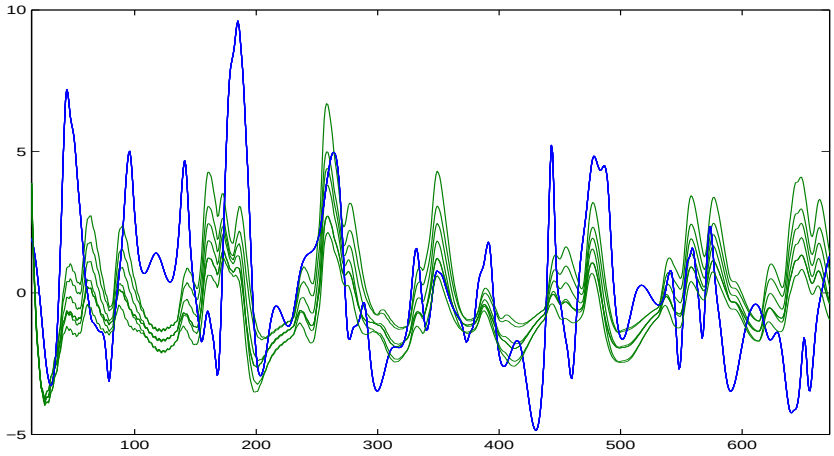

Figure 6.30: Simulated data using inputs varied ±25%.

This transformation was also used in these models, but without success.

6.3.2 NARMAX

Looking at the coherence plots in Fig. 5.12 there seems to be a poor linear relation between the inputs and the output. To overcome this it is possible to apart from using the ordinary glucose and insulin inputs take non-linear transformations of them and use as regressors. Systematically this is done using for example neural networks or radial basis functions. It is also possible to use other variables which lack obvious physiological explanation as regressors. One such variable is the time of the day. As mentioned in the physiology chapter the dynamics of the system is believed to vary over the day. Basically any variable believed to affect or correlate with the output may be used to try to explain the behavior of the output. Except from transforming the inputs by non-linear functions they may be for example multiplied creating new bilinear variables to use as input.

For the models presented above the following simple non-linear functions have been tried to create new inputs:

$$u_{i,j} = u_1^i u_2^j \qquad i,j = \{0 \dots 3\} \tag{6.9}$$

The time of the day was also tried as an input. None or insignificant improvement could be seen.

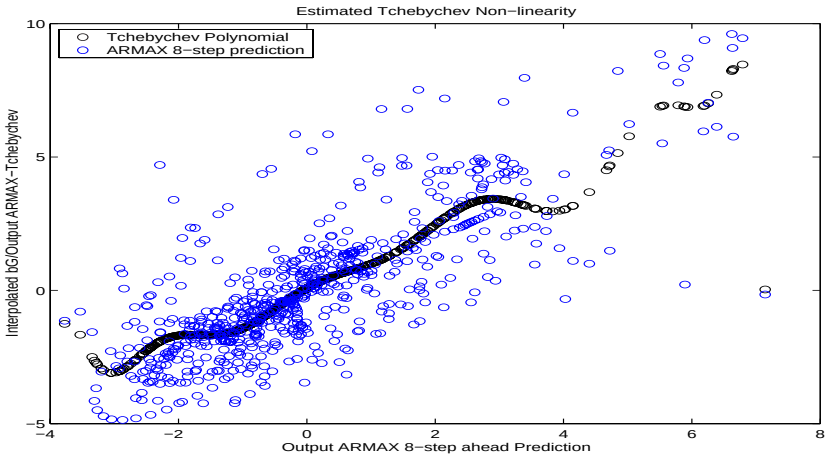

Figure 6.31: Chebychev Non-linearity and ARMAX 8-step ahead prediction.

6.3.3 GTFM-Wiener

The linear model can be extended by a non-linear function on the output. Such a model is called a Wiener model:

$$A(q^{-1}) \cdot y(t) = \frac{B_1(q^{-1})}{F_1(q^{-1})} \cdot u_1 + \frac{B_2(q^{-1})}{F_2(q^{-1})} \cdot u_2 + \frac{C(q^{-1})}{D(q^{-1})} \cdot e(t) \quad (6.10)$$

$$z(t) = h(y(t)) \quad (6.11)$$

where h(y(t)) is a non-linear function. Here Chebychev polynomials have been used to represent the this function. Polynomials of order 1-25 have been tested and evaluated using the Akaike criteria. The best polynomial according to Akaike is of 12:th order and can be seen in Fig. 6.31 together with the a plot of the GTFM 8-step predictions versus the splined data.

Prediction

Using this polynomial the prediction now improves somewhat as can be seen in Fig.6.32.

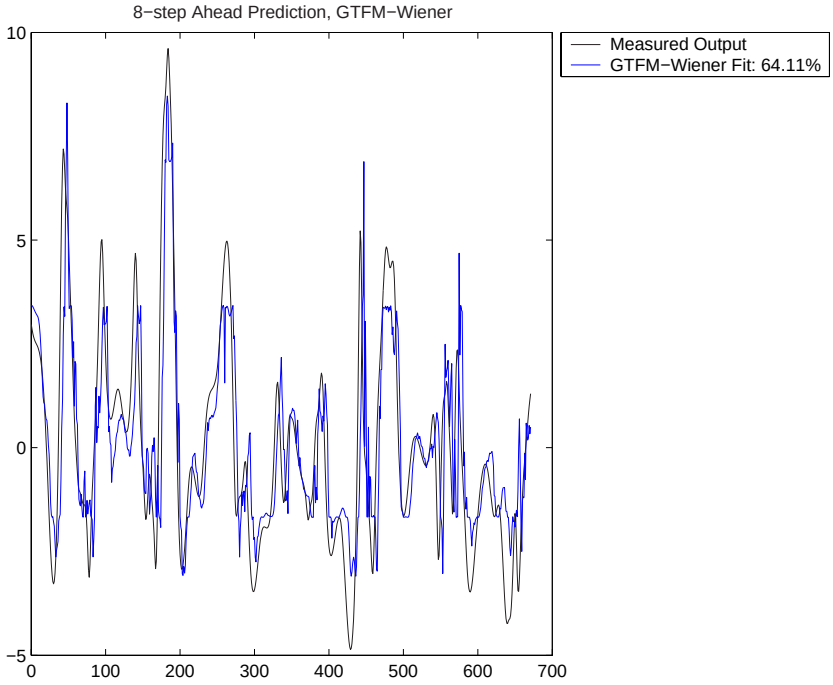

Figure 6.32: 8-step ahead prediction, GTFM-Wiener.

Chapter 7

Discussion

The problem of modelling diabetes has many difficulties. In this chapter a discussion of the difficulties encountered during this thesis will follow.

7.1 Validity

The data used in this thesis was collected from a newly diagnosed IDDM patient. The fact that only data from one patient was used raises the question of validity for the application of the results in other patients. Many of the problems and properties with the studied system are however general and relevant for modelling of other diabetics as well.

7.2 Data

First the issue of interpolating the scarce data was subjected. The data was sampled at an average of 9.3 samples/day. Assuming that 8 hours a day is spent sleeping when no sampling is undertaken, this corresponds to a sampling period of approximately 100 min. These samples were interpolated using a least squares splining method to get a sampling rate of 15 min. The spectrum of the sampled and interpolated signal was compared with the spectrum of an average of patients monitored by MiniMod, a sampling device collecting samples every fifth minute. The MiniMod samples were also resampled at different rates up to every third hour and interpolated using the same method as for the meter monitored data to get samples every 15 min. The spectra of these new signals were also compared to the interpolated data. The spectrum of the interpolated data falls between the spectra of the signal sampled at 60 min and the signal resampled at every 120 min. These signals were compared to the original signal and evaluated according to their ability to resemble the original signal. The 60 min signal has little trouble following the original signal. The 120min signal on the other hand misses the most rapid oscillations and has a significantly higher maximum

error. The interpolated data has an average sampling rate of every 100 min. The rapid changes in blood glucose concentration are often experienced as hypoglycemia and thus calls for sampling to establish glycemic status. Thus the rapid changes are often captured in these extra, unscheduled samples. Considering these aspects it may not be totally inadequate to say that these interpolated data are fair representations of the true data. This of course has to be subjected to further research where MiniMod samples are collected and compared to interpolated glucose meter samples for a large population. Thus an optimal sampling schedule and a robust and correct interpolation technique can be constructed.

7.3 Identifiability Issues

The only quantity of the system accessible to measurements is the blood glucose concentration. Glucose flux from the absorbtion of meals and the insulin absorbtion from the subcutaneous depots are not possible to measure directly. This poses a severe difficulty in the estimation of the sub-models and theirs outputs impact on the GIIM. The absorbtion of rapid-acting insulin and the glucose flux from carbohydrate intake are almost always present at the same time, making it difficult to access the influence of each input. A meal consists of both fast and slow carbohydrates obstructing the possibility/frsk to separate the dynamics of the two sources. This problem is difficult to avoid, since separating the insulin injections and carbohydrate intake creates unacceptable risks for the patient. This is undoubtly one of the major problems with trying to model and estimate the system under these conditions. The only possibility to get reliable estimates of these sub-models is to conduct clinical experiments such as glucose clamp techniques or tracer methods. Such experiments are cumbersome and not appropriate for routinely use.

7.4 The Sub-Models

The energy intake has been considered to consist of solely slow and fast carbohydrates. This is of course not true. Food consists two other major sources of energy, fat and protein. These can not be converted to glucose directly, but can be metabolized into glucose and FFA[1] in for example the liver in the post-absorbative stage. Therefore they also have an impact on the metabolism of the body, and thereby directly and indirectly on the GIIM. Regarding carbohydrates there is a vast spectra of different mono-, di- and polysaccharides and to simply divide their absorbtion dynamics in two categories is probably an over-simplification.

[1] Free Fatty Acids; can be used by some cells as fuel

The fast carbohydrates were modelled using a second order compartment model. Looking at the absorbtion profile from[34], this seems to be a plausible model to represent the absorbtion. The slow carbohydrates were modelled using a fourth order compartment model. Slow carbohydrates first have to be digested into glucose before absorbed and therefore have a delay between intake and absorbtion. The fourth order compartment model creates such a delay in the absorbtion. As mentioned above, fat and protein have not been regarded. Apart from providing energy they influence the absorbtion dynamics.

The GSM used in this thesis has been kept very simple for a number of reasons. Firstly this thesis is about the entire glycemic system and a thorough modelling would simply take too much effort. Secondly the information about the contents of the meals is rather scarce in the diabetes diary. Meals are simply noted as breakfast, lunch, dinner and an estimate of their size; small,normal or large. Thirdly the accuracy in the model has to stand in proportion to the accuracy of the inputs. Notes on the exact amounts of carbohydrates, protein and fat in the diary is simply not realistic.

Whether these simple models are too simplified to describe the absorbtion in a acceptable way remains to be investigated. Most likely research has to be targeted at physiological modelling and understanding of how the digestive and absorbative processes are influenced by the composition of the meals. However it has to be borne in mind that the data available can not be assumed to very accurate. For this effort also has to be put on developing simple and accurate ways to estimate the content of a meal. In Australia food producers can now have their products measured with the glycemic index analysis and labelled with the glycemic index on the package. Thereby the consumers can easily get an estimate of the glycemic effect of the product. Glycemic Index is a debated issue, and has some serious shortcomings in describing the absorbtion profile of meal. For a review of glycemic index and its pro's and con's see [26, 35, 21, 37, 27, 20, 42].

The ISM has been modelled using a second order compartment model for the rapid-acting insulin and the Berger model for the slow-acting insulin. The rapid-acting insulin has a very fast onset, which the second order model is able to represent. The dynamics of the slow-acting insulin is widely considered to be dose-dependant. This makes compartment model unsuitable, since they are linear. Instead the Berger model was used to represent the dynamics. The non-linear nature of the Berger model makes it difficult to estimate and therefore parameter values found in the literature were used. This is of course not optimal since these average parameter values likely differ from those representing this specific patient. The absorbtion of the slow-acting insulin is however too slow to seriously affect the essential dynamics of the system following a meal.

The sub-models were estimated using the Matlab tool PEM, found in the system identification toolbox. The result of this estimation process ended

with parameter values lying quite close to the initial values. Considering this and taking the identification difficulties mentioned above into consideration these results should be viewed with some scepticism.

7.5 Unrepresented Inputs

The modelling has been based on measurements and estimates of blood glucose, size and timing insulin injection doses and meals. There may however be other inputs that have an important influence on the dynamics of the system. One such input may be physical exercise. Apart from having a blood glucose lowering effect due to the utilization of glucose in the muscle cells, exercise also has a positive effect on insulin sensitivity. Thus the effect of insulin is also enhanced. This variable has not been considered mainly due to difficulties in quantifying it properly. An other variable of interest is the time of the day. The dynamics of the system is believed to vary over the day, especially during the morning compared to the rest of the day. In this thesis this variable has simply been tried as a regressor, but without much success. An alternative would be to divide the day in different segments and have multiple sets of parameters, one set for each segment. Finally alcohol intake also has to be considered as a specific input. The metabolism of alcohol disturbs the endogenous glucose production, and thus has a glucose lowering effect. This variable has not been subjected either. This is mainly due to that such consumption has not been noted in the diary.

7.6 The Linear Models of GIIM

Three different types of models were investigated, an ARMAX-model, subspace models and the GTFM. Of these the GTFM proved to best represent the system. The ARMAX model and the GTFM were quite similar both with regards to prediction and their Bode plots. THe subspace models differed significantly from the two others with resonance peaks in the GSM/GIIM transfer function at high frequencies. All models shared some features though. For the ISM/GIIM transfer function all models had a pole pair close to $0.85 \pm 0.1i$. Likewise they all agree that the GSM/GIIM transfer function has a pole pair in the area $0.5 - 0.8 \pm 0.5 - 0.7i$. This may indicate that these dynamics are essential parts of the system.

The 8-step prediction was quite poor for all the models. The models had difficulty with the high peaks and the low bottoms of the data. This is probably an artefact of non-linearities in the system, but can also be due to that the gains of the GIIM are underestimated due to that the inputs cancel each other as discussed above. This problem can be seen even clearer in the simulation of the GTFM. By simply scaling the output the simulated output resembles the true data at some periods. In other segments of the

data the model is completely out of track. The poor simulation result can be explained by a number of factors. Firstly that the interpolated data that the model tries to represent is flawed. Secondly that the inputs used for simulation may be flawed. Thirdly and finally that the model is poorly estimated and/or that the model structure is inadequate to represent the system. Most likely it is a sum of all these factors. Most of these problems have been discussed above, except the question of whether the linear models are adequate enough to represent the system. This will be subjected next.

7.7 Non-linearity

Looking at the coherency plots between the insulin and glucose input to the GIIM and the glucose output it seems to be a poor linear relationship between these variables. This may in part be explained by that there are unrepresented inputs that have a significant impact on the glucose concentration. Even if so the coherence ought to be higher if the GSM/GIIM- and ISM/GIIM-relation could be modelled linearly, since these variables undoubtedly are the most important inputs.

A simple way to make the system non-linear is to transform the data. In the data chapter the log-normal nature of the blood glucose samples was reviewed. Looking at the log-normal plot in Fig. it seems very plausible to say that the blood glucose data is log-normally distributed. Therefore a natural transformation would be to take the natural logarithm of the data. This transform and the transform suggested by Kovatchev were tested on the linear model without improvement. The coherence plots did not improve either. Instead some simple Hammerstein and Wiener models were considered to extend the GTFM. The Hammerstein models used did not improve the model performance. The Wiener model used was a Chebychev polynomial. The accuracy of the prediction improved somewhat with this model.

7.8 Time-Varying Dynamics

The dynamics of the system vary not only over the time of the day, as discussed above, but also in a longer time span. This is especially evident in the studied data period. In Fig. the parameter values of the Matlab algorithm SEGMENT can be seen. SEGMENT estimates a recursive ARMAX-model for the entire data period and in the plot the variation of these parameters over the period can be seen. The parameters fluctuate very much and then stabilize in the end. The fact that the parameters seem to stabilize may indicate the end of the honey-moon period. The variations in the system dynamics are normally not as rapid and violent as this data, but there are variations due to continuous β-cell destruction, variations in body mass,

level of exercise etc. It is therefore important to remember that no model is valid forever, but has to be recursively estimated, so that it corresponds to the present dynamics.

Chapter 8

Conclusion

The purpose of this thesis was to develop and evaluate different models of IDDM, based on one patient's data. The aim was to be able to predict blood glucose values two hours ahead with an prediction error smaller than 1 mmol/l in 95 % of the cases. The best model, the GTFM-Wiener model did not meet this goal. The reasons for this are several:

- The number of measurements may be too few and the interpolation method not optimal, resulting in a poor reconstruction of the blood glucose curve.
- The system was hard to identify using this data. The inputs act simultaneously, making it difficult to estimate the sub-models and to extract the specific impact of each input on the output.
- The system is non-linear and can thus not be represented by the linear models.
- The sub-models used to describe the glucose flux and the insulin absorbtion are probably too simple to accurately describe these processes.
- The estimates of the size and timing of the meals and insulin injections are not very accurate.
- Unrepresented variables are probably relevant to describe the system. Such inputs may be exercise and alcohol intake.

Apart from these difficulties some other interesting properties of the system are:

- The system dynamics are time-varying especially during the honeymoon phase.
- The glucose measurements are log-normally distributed.

- All the linear models had some common dynamics. This may indicate that these dynamics are essential to the system.

This thesis did not meet the goals set, but hopefully revealed some interesting features and some of the inherent difficulties of modelling this system. Much effort has to be put at analyzing these issues. A brief survey of possible further research can be found in the next chapter.

Chapter 9

Further Research

In this chapter some ideas for further research are briefly presented.

- **Optimal Sampling Schedule:** Blood glucose sampling conducted with a glucose meter is costly and constitutes a annoyance for the patients. For these reasons the sampling has to be effective. Thus, one research object is to evaluate how many samples, and when these are to be taken, to be able to reliably reconstruct the blood glucose curve.
- **Reconstructing the blood glucose curve:** Given these samples, an effective interpolation algorithm and predictive filter has to be available to reconstruct the blood glucose curve.
- **Modelling the Subsystems:** As seen in this thesis the sub-models are very important to accurately describe the system. Flaws in the sub-models can not be corrected in the GIIM. Especially the GSM is difficult to model, and must be analyzed with regards to the influence of fat, protein and fiber on the dynamics of the digestive and absorbative processes.
- **Hammerstein-Wiener models using EKF:** The system is non-linear, and thus calls for non-linear models. One such concept that may be tested is the Hammerstein-Wiener approach, identified using the extended Kalman filter[31].
- **Physiological Modelling** For a deeper understanding of the dynamics of this system, a physiological model is indispensable. C. Cobelli is currently working on such a model[16], based on previous modelling efforts[15, 9].
- **Exercise:** Exercise probably has an important effect on the dynamics of the system, directly in terms of disposal of glucose, but also indirectly through the effects on the insulin sensitivity. These mechanisms must be subjected both theoretically and experimentally.

- **Time-varying dynamics:** The time variations over the elapse of the day has to be considered carefully. If the dynamics shift over the day, different parameter sets of the model has to be considered, one for each segment of the day, for which the parameters can be considered fixed.

Appendix A

Predefined Meals

In the diary the meals were noted using the semantic expressions small, normal and large. Below follows a definition of these standard meals in terms of fast and slow carbohydrate content. These definitions have been based on the patient's estimate of the amount ingested, the weighing of some groceries and by the use of [32].

Food	Fast(g)	Slow(g)	Total(g)
Breakfast, normal	10	45	55
Breakfast, small	10	25	35
Lunch, small	5	40	45
Lunch, normal	5	85	90
Dinner, normal	5	85	90
Dinner, large	10	120	130
Snack, small	0	10	10
Snack, normal	0	20	20
Dextrosol, 1 piece	3.5	0	3.5
Sweets, 10g	8	0	8
Apple	3	20	23
Pear	3	12	15
Banana	11	18	29
Peach	1	9	10
Potato Chips, 100g	0	47	47

Bibliography

[1] www.lilly.com.

[2] www.novonordisk.com.

[3] E. Ackerman, L.C. Gatewood, J.W. Rosevear, and G.D. Molnar. Model studies of blood-glucose regulation. *Bulletin of Mathematical Biophysics*, 27(Special Issue):pp. 21–37, 1965.

[4] Tom Arleth, Steen Andreasson, Marco O. Federici, and Massimo M. Benedetti. A model of the endogenous glucose balance incorparating the characteristics of glucose transporters. *Computer Methods and Programs in Biomedicine*, 62:pp. 219–234, 2000.

[5] Karl J. Åström and Björn Wittenmark. *Computer-Controlled Systems*. Prentice Hall, 3rd edition, 1997.

[6] R. Bellazzi, P. Magni, and G. De Nicolao. Baysian analysis of blood glucose time series from diabetes home monitoring. *IEEE Transactions on Biomedical Engineering*, 47(7):pp. 971–975, July 2000.

[7] R. Bellazzi, C. Siviero, M. Stefanelli, and G.D. Nicolao. Adaptive controllers for intelligent monitoring. *Artificial Intelligence in Medicine*, 7:pp. 515–540, 1995.

[8] Markus Berger and David Rodbard. Computer simulation of plasma insulin and glucose dynamics after subcutaneous insulin injection. *Diabetes Care*, 12(10):pp. 725–736, nov/dec 1989.

[9] R.N. Bergman and C. Cobelli. Minimal modeling, partition analysis, and the estimation of insulin sensitivity. *Federation Proceedings*, 39(1):pp. 110–115, January 1980.

[10] Geert-Jan Biessels. Cerebral complications of diabetes: clinical findings and pathogenetic mechanisms. *The Netherlands Journal of Medicine*, 54:pp. 35–45, 1999.

[11] Jens Brange and Aage Vølund. Insulin analogs with improved pharmocokinetic profiles. *Advanced Drug Delivery Reviews*, 35:pp. 307–335, 1999.

[12] T. Bremer and D.A. Gough. Is blood glucose predictable from previous values? a solicitation for data. *Diabetes*, 48:pp. 445–451, March 1999.

[13] M.R. Burge and D.S. Schade. Insulins. *Endocrinology and Metabolism Clinics of North America*, 26(3):pp. 575–598, 1997.

[14] E.R. Carson, T. Deutsch, H.J. Leicester, A.V. Roudsari, and P.H. Sonksen. Challenges for measurement science and measurement practice: the collection and interpretation of home-monitored blood glucose data. *Measurement*, pages 281–293, 1998.

[15] C. Cobelli and A. Mari. Validation of mathematical models of complex endocrine-metabolic systems. a case study on a model of glucose regulation. *Medical and Biological Eng. and Comput.*, 21:pp. 390–399, 1983.

[16] C. Cobelli, G. Nucci, and S. Del Prato. A physiological simulation model of the glucose-insulin system. *Proceedings of the first joint BMES/EMBS Conference*, page 999, 1999.

[17] C. Cobelli, R. Rizza, and et al. Use of a novel triple-tracer approach to assess postprandial glucose metabolism. *American Journal of Physiology*, pages E55–E69, 2003.

[18] Roche Diagnostics. *Accu-Check Compact Glucose*, 07 2001.

[19] S. Kodama F. Kajiya and H. Abe, editors. *Compartmental Analysis: Medical Applications and Theoretical Background*. Karger, 1984.

[20] S. Kaye Foster-Powell and J.C. Brand-Miller. International table of glycemic index and glycemic load values:2002. *The American Journal of Clinical Nutrition*, 76:pp. 5–56, 2002.

[21] M.C. Gannon and F.Q. Nuttall. Factors affecting interpretation of postprandial glucose and insulin areas. *Diabetes Care*, 10(6):pp. 759–763, Nov-Dec 1987.

[22] Michael Hanss and Oliver Nehls. Simulation of the human glucose metabolism using fuzzy arithemics. *Fuzzy Information Processing Society, 2000. NAFIPS. 19th International Conference of the North America*, pages 201–205, 2000.

[23] Bert Haverkamp. *Subspace Method Identification, theory and practice*. PhD thesis, Delft University of Technology, The Netherlands, 2000.

[24] L. Heinemann, C. Weyer, M. Rauhaus, S. Heinrichs, and T. Heise. Variability of the metabolic effect of soluble insulin and the rapid-acting insulin analog insulin aspart. *Diabetes Care*, 21(11):pp. 1910–1914, November 1998.

[25] P.D. Home. Insulin therapy. *International Textbook of Diabetes Mellitus*, pages 899–928, 1997.

[26] D.J.A. Jenkins, T.M.S. Wolever, and A.L. Jenkins. Starchy foods and glycemic index. *Diabetes Care*, 11(2):pp. 149–159, February 1988.

[27] TMS Wolever DJA Jenkins. The use of the glycemid index in predicting the blood glucose response to mixed meals. *The American Journal of Clinical Nutrition*, 43:pp. 167–172, 1986.

[28] Rolf Johansson. *System Modeling and Identification*. Prentice Hall, 1st edition, 2002.

[29] C.R. Kahn. Insulin receptors and insulin signaling in normal and disease states. *International Textbook of Diabetes Mellitus*, pages 437–467, 1997.

[30] BP Kovatchev, DJ Cox, LA Gonder-Frederick, and WL Clarke. Symmetization of the blood glucose measurement scale and its applications. *Diabetes Care*, 20:pp. 1655–1658, 1997.

[31] M. Kozek and N. Jovanovic. Identification of hammerstein/wiener nonlinear systems with extended kalman filters. *Proceedings of the American Control Conference*, pages 969–974, 2002.

[32] Livsmedelsverket. *Livsmedelstabell — Energi- och Näringsämnen 2002*. Livsmedelsverket.

[33] Lennart Ljung. *System Identification: Theory for the User*. Prentice Hall, second edition, 1999.

[34] Chiara Dalla Man, Andrea Caumo, and Claudio Cobelli. The oral glucose minimal model: Estimation of insulin sensitivity from a meal test. *IEEE Transactions On Biomedical Engineering*, 49(5):pp. 419–429, May 2002.

[35] J.C. Brand Miller. Importance of glycemic index in diabetes. *American Journal of Clinical Nutrition*, 59(suppl.):pp. 747–752, 1994.

[36] Gianluca Nucci and Claudio Cobelli. Models of subcutaneous insulin kinetics. a critical review. *Computer Methods and Programs in Biomedicine*, 62:pp. 249–257, 2000.

[37] F Xavier Pi-Sunyer. Glycemic index and disease. *The American Journal of Clinical Nutrition*, 76(suppl.):pp. 290S–298S, 2002.

[38] S. Sasaki. Mechanism of insulin action on glucose metabolism in ruminants. *Animal Science Journal*, 73:pp. 423–433, 2002.

[39] Steven E. Shoelson and Philippe A. Halban. Insulin biosynthesis and chemistry. *Joslin's Diabetes Mellitus*, pages 29–55, 1994.

[40] A. Vander, J. Sherman, and D. Luciano. *Human Physiology.* McGraw-Hill, 8th edition, 2001.

[41] M.F. White and C.R. Kahn. Molecular aspects of insulin action. *Joslin's Diabetes Mellitus*, pages 139–162, 1994.

[42] D. R. L. Worthington. Minimal model of food absorbtion in the gut. *Medical Informatics*, 22(1):pp. 35–45, 1997.

[43] D.R.L Worthington. The use of models in the self-management of insulin-dependant diabetes mellitus. *Computer Methods and Programs in Biomedicine*, 32:pp. 233–239, 1990.